SELF-ASSOCIATION IS A COMMON PROPERTY IN BOVINE, MOUSE AND *XENOPUS* ARRESTIN

Shuang Qiu

A master thesis in

Department of Neuroscience and Physiology

Submitted in partial fulfilment of the requirements for the degree for Master in Science in College of Graduate Studies of State University of New York, Upstate Medical University

Approved by_____

(Sponsor's Signature)

Date _____

ACKNOWLEDGEMENTS

First and foremost, I would like to acknowledge my thesis advisor, Dr. Peter Calvert, for support and advice. I appreciate the time he spent on experimental guidance, editing my thesis and helping me with my presentation.

I would also thank Stephen Shinsky, Anamika Patel and Dr. Michael Cosgrove for performing analytical ultracentrifugation experiments.

Special thanks go to my thesis committee members, Dr. Michael Cosgrove, Dr. Eric Olson, Dr. Eduardo Solessio and Dr. Peter Calvert. I want to especially thank them for finding time in their busy schedules to review this thesis and provide suggestions, constructive and critical comments.

I would like to thank members of my laboratory as well as the faculty and staff in the College of Graduate Studies, Department of Neuroscience & Physiology and Center for Vision Research.

Finally, I would like to thank my friends and family for their support in my study at SUNY Upstate Medical University.

ABSTRACT

The light-driven translocation of arrestin from rod inner segment to outer segment was indicated to involve free diffusion with binding affinity to light-activated phosphorhodopsin, however, it is still debatable how arrestin is excluded from the dark-adapted outer segment. Previous studies demonstrated that bovine visual arrestin had the property of self-association. The self-association property of both wild-type and mutated purified visual arrestin of several species (bovine, mouse and *Xenopus laevis*) was studied by performing analytical ultracentrifugation experiments which provided the oligomer formation information and association constants. The self-association parameters of purified bovine and mouse visual arrestin were investigated and compared with other studies. Results showed that arrestin of both species could self-associate, forming dimers in a concentration-dependent manner, but tetramers were not detected at the highest concentrations examined. *Xenopus* arrestin was shown to self-associate as well, existing in a monomer-dimer equilibrium with the dimer dissociation constant $K_{D,dim}$=80.8 μM, which suggested that self-association was also a feature of *Xenopus* visual arrestin. Interestingly, homologous mutations (F78A/Y84A/F193A) of *Xenopus* arrestin, which were supposed to be constitutive monomers, failed to completely disrupt the oligomerization of *Xenopus* arrestin with the dimer dissociation constant $K_{D,dim}$=200.7μM , indicating that these regions were not conserved in amphibian visual arrestin, including *Xenopus laevis*. The percentage of the dimer was higher than that of monomer at physiological concentrations in all species of arrestins tested.

TABLE OF CONTENT

CONTENTS

LIST OF TABLE AND FIGURE

LIST OF ABBREVIATION

ATP	Adenosine Triphosphate
AUC	Analytical Ultracentrifugation
CC	Connecting Cilium
cGMP	Cyclic Guanosine Monophosphate
EGFP	Enhanced Green Fluorescence Protein
ER	Endoplasmic Reticulum
ERG	Electroretinogram
GPCR	G-protein Coupled Receptor
GDP	Guanosine Diphosphate
GTP	Guanosine Triphosphate
IS	Inner Segment
OS	Outer Segment
PAGFP	Photoactivatable Green Fluorescent Protein
REMI	Restriction Enzyme Mediated Integration
SASX	Small Angle X-ray Scattering
SDS-PAGE	Sodium Dodecyl Sulfate Polyacrylamide Gel Electrophoresis
WT	Wild Type

CHPATER 1 INTRODUCTION

1.1. Photoreceptors and Phototransduction

Eyes are fluid-filled spherical organs composed by three concentric layers, among which, the inner layer, named “retina”, contains light-sensitive, sensory neurons. The retina contains five classes of neurons: photoreceptors, bipolar cells, ganglion cells, horizontal cells and amacrine cells (Fig.1). Photoreceptor-bipolar cell-ganglion cell forms the major route of visual information flow.

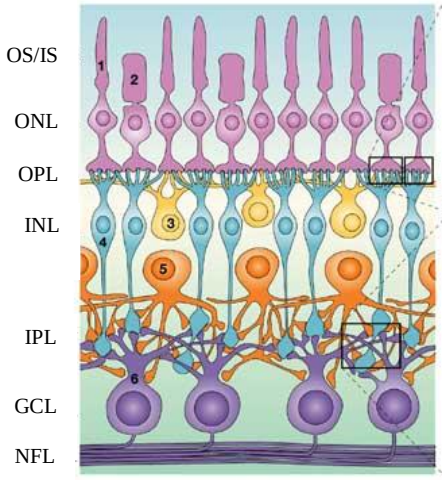

Figure 1 Schematic of the mammalian retina [1]. Five types of neurons: photoreceptors (rods (1), cones(2)), horizontal cells (3), bipolar cells (4), amacrine cells(5) and retinal ganglion cells (RGCs) (6). (OS/IS, outer and inner segments of rods and cones; ONL, outer nuclear layer; OPL, outer plexiform layer; INL, inner nuclear layer; IPL, inner plexiform layer; GCL, ganglion cell layer; NFL, optic nerve fibre layer).

The photoreceptor is a sensory neuron with a distinct design: it is composed of the outer segment (OS), the inner segment (IS), and the synapse [2]. The photoreceptor, located in the outer layer of the retina, converts light into electrical signals through a cascade of biochemical reactions. Phototransduction cascade occurs in the outer segment, and members in phototransduction process, including rhodopsin, are synthesized in the inner segment, which

contains organelles such as ribosomes and mitochondria [2]. Based on their shapes, photoreceptors could be divided into two types: cones and rods. In particular, cones are named after their cone-shaped outer segment, while rods possess long cylindrical-shaped outer segment [2]. Cones are significantly responsible for brighter light and color vision, while visual experience at low light levels is mostly attributed to rods [3, 4].

1.1.1 Rod Photoreceptor Structure

Outer and inner segments comprise the major rod photoreceptor structure, and they are connected by the cilium with the diameter of only 0.25-0.3 μm [5]. The rod outer segment, which is a primary cilium adjusted into a functional organelle involved in light absorption, contains thousands of disk membranes [6] that occupy half volume of the outer segment [7]. The disk membranes contain light-sensitive photopigment rhodopsin as well [8]. By contrast, the inner segment (or cell body) is less densely populated, and is composed of diverse subcompartments related to homeostasis of the cell and phototransduction proteins synthesis. The inner segment mainly includes three compartments: ellipsoid, which contains mitochondria for the regulation of cellular metabolism [9]; myoid, which possess Golgi apparatus, rough endoplasmic reticulum and smooth endoplasmic reticulum [9, 10]; and nucleus, which is located before pre-synaptic region where information is passed from photoreceptor cells to bipolar cells [11].

1.1.2 Phototransduction Cascade & Light Response

In most sensory systems, activation of receptors usually leads to the depolarization of cell membranes and stimulates an action potential. The study performed by Toyoda et al [12] showed that in the dark, the photoreceptors are in the depolarized state with the membrane potential of -35 to -40 mV. They also discovered that the intensity of light caused a graded change in

membrane potential and hyperpolarized the membrane, reaching about -70 mV. As a result, unlike most neurons in central nerves system which depolarize when stimulated, photoreceptor cells oppositely behave, tending to hyperpolarize instead [13]. In the outer segment, the cyclic guanosine monophosphate (cGMP) level is responsible for the regulation of opening and closing of the cGMP-gated channels. In the dark, the inward current of Na^+ and Ca^{2+} through cGMP-gated channels is opposed by an outward current regulated by noninactivating potassium-selective channels in the inner segment. The influx of Na^+ and Ca^{2+}, coupled with the efflux of the potassium ion (K^+), contributes to the dark current and keeps the photoreceptor in a depolarized state [14]. Light absorption decreases cGMP concentration in the outer segment, leading to the closure of cGMP-gated channels in the outer segment, and the reduction of Na^+ and Ca^{2+} influx. The closure of cGMP-gated channels and the decrease of positive charge influx break the homeostasis of the current loop between cGMP-gated channels and potassium channels, leading the intracellular voltage to become more negative and the hyperpolarization of the cell (Fig.2) [15].

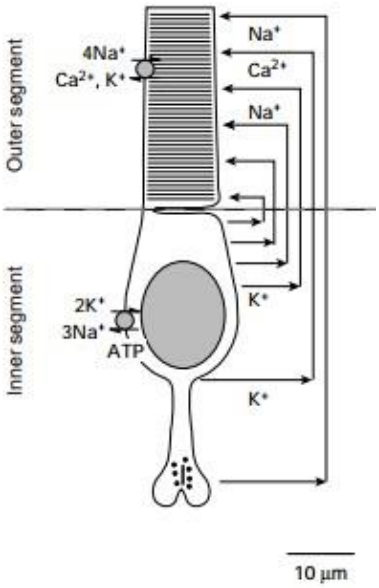

Figure 2 Nature of circulating current in rod photoreceptor [15].

Rhodopsin, the photopigment in rods, is composed of opsin and retinal. The retinal molecule is located in the pocket formed by the seven transmembrane domains of opsin, which traverse the disk membranes in rod outer segment. Absorption of light results in the break of one double bond between two carbon atoms of retinal, changing 11-*cis* retinal into all-*trans* retinal. Such transformation activates the intracellular messenger transducin by exchanging GTP in place of GDP on the transducin α subunit, followed by the separation of α subunit from βγ subunit. The binding of the GTP-bound transducin α subunit to cGMP phosphodiesterase increases the cGMP hydrolysis rate. The resulting reduction in cGMP concentration leads to the closure of the channels in the outer segment plasma membrane [16].

Once the activation is initiated, the inactivation process also starts rapidly, including the phosphorylation of activated rhodopsin by rhodopsin kinase and the binding of arrestin to rhodopsin. Bound arrestin restrains the ability of rhodopsin to stimulate transducin, blocking the activation of transducin and cGMP phosphodiesterase. The activity of rhodopsin kinase is regulated by recoverin, which is a Ca^{2+}-binding protein and inhibits rhodopsin kinase at high Ca^{2+} concentration [16] (Fig.3).

(A) Cascade activation

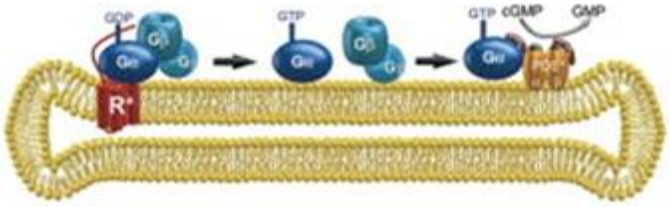

(B) Rhodopsin inactivation

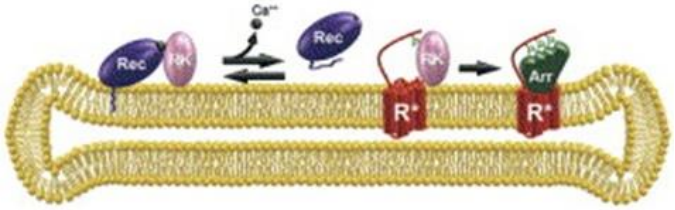

(C)

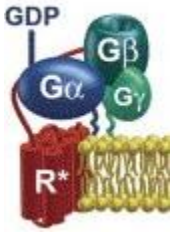

Figure 3 Phototransduction cascade in rod photoreceptors [16]. (A) Phototransduction cascade activation. (B) Rhodopsin inactivation. (C) Transducin αβγ hetrotrimer with a myristoyl group on α subunit and a farnesyl group on βγ subunits

1.1.3 Light Adaptation and Calcium Regulation in Photoreceptors

Generally speaking, light adaptation contains all changes in rod photoreceptor sensitivity which take place as a result of increasing illumination levels [17]. After the photoreceptor absorbs a single photon, ~5% of the open, light-sensitive cGMP channels become closed in ~1s, indicating that all of the channels will be closed if ~100 photons are delivered per second [18]. Due to light adaptation, however, this would not happen until ~10,000 photons are absorbed per second [18].

Ca^{2+} is one of the major messengers for eukaryote cell activity regulation [19]. It functions as a control and regulation ion to a variety of eukaryote cell types including animals, plants and fungi [20]. The Ca^{2+} concentration inside the cell is regulated through the balance between the ions influx and efflux [21]. In the dark, the Ca^{2+} influx is balanced by its efflux

through the Na^+/Ca^{2+}-K^+ exchanger, which has four Na^+ into the cell with one K^+ and one Ca^{2+} out of the cell. Hence, in darkness, the Ca^{2+} concentration inside the cell is ~500 nM [22], which is high enough for the regulation of phototransduction cascade in rod outer segment and transmitter release in rod inner segment [20]. After the absorption of light, the influx of Ca^{2+} ion stops because of the closure of cGMP-gated channels, however, its efflux through the Na^+/Ca^{2+}-K^+ exchanger still continues [23, 24], which as a result decreases the Ca^{2+} concentration to at least 50 nM [25].

In photoreceptors, the cGMP concentration inside the cell is determined by both its synthesis rate, which is controlled by guanylate cyclase, and its hydrolysis rate, which is regulated by cGMP phosphodiesterase (PDE) [26]. In the dark, cGMP remains at a steady state with the concentration of several micromolar, which keeps the cGMP-gated channels in the outer segment open and photoreceptor cells stay at a depolarized state [18]. For years, Ca^{2+} has been regarded as the major factor in light-adaptation because of its regulation of several components in phototransduction cascade and the decrease of Ca^{2+} concentration contributes to the recovery and adaption processes [27-29]. Rod photoreceptors are sensitive to low level of light, but the sensitivity decreases when the intensity of illumination increases, deterring the photoreceptors from saturating. In the process of light adaptation, the Ca^{2+} concentration in the photoreceptor outer segment is a major factor in the regulation of photoreceptor sensitivity to light. Firstly, the activity of guanylate cyclase is inhibited by the high calcium concentration in the photoreceptor outer segment. This regulation of guanlate cyclase occurs via guanlyl cyclase activating proteins (GCAP-1 and GCAP-2), which is a type of Ca^{2+} binding protein and is in the inactivated state when binding to Ca^{2+} [30]. Illumination leads to the closure of cGMP-gated channels in the photoreceptor outer segment, reducing the Ca^{2+} concentration and further increasing the activities

of guanylate cyclase, hence increasing the cGMP level [18]. Secondly, the decrease of Ca^{2+} concentration results in higher sensitivity of the cGMP-gated channels to cGMP through the action of calmodulin or calmodulin-like proteins, promoting the binding of cGMP-gated channels and cGMP [31]. In the dark when Ca^{2+} concentration is high, calmodulin binds to the β-subunit of the cGMP-gated channel and the channel has low affinity to cGMP. When photoreceptors absorb light, calmodulin dissociates from the channels, leading to the higher affinity of the channel to cGMP [29]. Thirdly, Ca^{2+} also plays a role in the regulation of visual pigment sensitivity. The activity of rhodopsin kinase is regulated by recoverin, which is a Ca^{2+}-binding protein and inhibits rhodopsin kinase at high Ca^{2+} levels. As a result, the rhodopsin kinase activity increases with the decrease of Ca^{2+} concentration as well, allowing arrestin to bind rhodopsin more rapidly due to the enhancement of rhodopsin phosphorylation via the action of recoverin, and finally causing the decrease of the signaling lifetime [27, 32].

1.1.4 Light-dependent translocation of signaling proteins

In 1980s, several laboratories discovered a significant change in transducin and arrestin localization in rod photoreceptors [33-35]. In dark-adapted rods, the outer segment contains little amount of arrestin which is mostly localized in the inner segment. Arrestin, which is involved in the inactivation of rhodopsin, moves to and accumulates in the outer segment in response to light [33]. Transducin moves in the opposite direction. It is localized to the rod outer segment in dark-adapted status and translocates to the inner segment upon light exposure [16, 34-36]. In addition, a third signaling protein, recoverin, moves from the rod outer segment towards the synapse [37] (Fig.4). Hence, in the bright light, most arrestin stays in the outer segment binding to rhodopsin and dampens the receptor signaling pathway that triggers the cellular response [38]. Arrestin knockout mice are shown to cause light-dependent rod death, demonstrating the important

function of arrestin translocalization in rod survival and protecting rods from light-induced cell death [39, 40]. The mechanisms underlying this light-driven translocation will be discussed in detail in the Section 1.2 .

Protein redistribution probably contributes to photoreceptor light adaptation by regulating the sensitivity and speed of photoresponse to different light conditions [41]. It could be mostly elucidated by the fact that both light adaptation and protein translocation can occur in a light-dependent manner at the same time [17]. Previous research showed that the light-dependent translocation of transducin between rod subcellular compartments might be a mechanism of light adaptation, because the decrease of transducin content in the outer segment was accompanied by the decrease in amplification of photoresponse [17]. In addition, observation was made that the ability of light adaptation was disrupted in the G_{γ} mutant knockin mice [42]. The mutant mice had a tight binding of $G_{\beta\gamma}$ to membranes and hence prevented the translocation to rod inner segment, further demonstrating that transducin translocation might have the function of light adaption. Rod photoresponse is dependent on the activation of transducin, and the translocation of transducin from the outer to inner segment decreases its concentration in the outer segment and therefore, lowers the rate of transducin being activated [41]. The photoresponse sensitivity is decreased as well and the photoresponse saturating will be prevented. The time course of transducin translocation from outer segment to inner segment was shown to be 5 min for G_{α} subunit and 12.5 min for $G_{\beta\gamma}$ subunits, and the movement of the two subunits back to the outer segment needed 2.5 h [17]. Following a similar time course as transducin, significant translocation of arrestin took 5-6 min from dark to light and 30 min from light to dark [37, 43]. Moreover, the number of translocating arrestin is superstoichiometric to the amount of activated rhodopsin, with the ratio of ~30:1 [37]. The increasing rate of arrestin binding to phosphorylated

photoactivated rhodopsin decreases the transducin amount being activated and lowers photoresponse sensitivity. In addition, arrestin translocation increases the rate of photoresponse shutoff and leads to a reduction in the lifetime of activated rhodopsin [41]. However, no direct evidence has been shown whether arrestin translocation has a significant task during light adaptation.

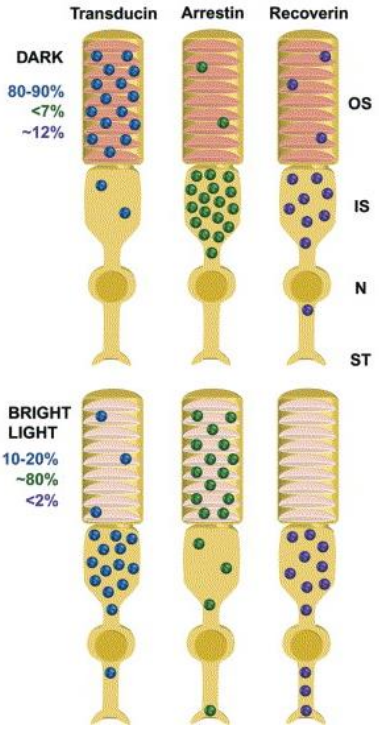

Figure 4 Schematic illustration of transducin, arrestin and recoverin distribution in dark-adapted and light-adapted rods [16].

1.2. Light-Dependent Distribution of Phototransduction Proteins and mechanisms

1.2.1 Light-Dependent Translocation of Transducin

Previous literature demonstrated that transducin translocation was regulated by the diffusion with binding partner, and the differences of membrane affinities of transducin hetertrimeric complex before and after dissociation could explain this phenomenon [17, 42, 44-47]. The transducin heterotrimer exists in the rod outer segment by the combined action of its α

subunit with a myristoyl group and βγ subunits with a farnesyl group. Absorbing light leads to the binding of transducin α subunit with GTP and the dissociation from βγ subunits, which finally makes the subunits more soluble and easier to escape from the outer segment and diffuse into the inner segment. People have speculated that if GTP hydrolysis occurs in the rod inner segment, it will lead to the time of the transducin subunits separated from each other being short, and make the subunits reform as hetertrimeric complex and bind to the membranous structures in the inner segment [16]. Also, overexpression of the GTPase activating protein RGS9 [48] disrupted the translocation of transducin [49]. In agreement with the observation, the transducin translocation was faster in RGS9 knockout mice than wild-type ones because of its lower inactivation rate [50]. The translocation rates of transducin α subunit and βγ subunits are different [17], indicating that they travelled to the inner segment separately [16]. Kassai et al also stated that transducin βγ subunits translocation was interrupted without affecting the movement of α subunit when they substituted a geranylgeranyl group for the farnesyl group, hence increasing the membrane affinity [42]. Phosducin, which could bind transducin βγ subunits and prevent their association with α subunit, was shown to enhance the translocation of transducin [45]. Additionally, it decreased the membrane affinity by masking the farnesyl residue of βγ subunits [51] and diminishing the electrostatic interactions between βγ subunits and membrane phospholipids with negative charge [52]. People also observed that phosducin was located throughout the entire rod cytoplasm and the translocation of transducin βγ subunits was disrupted in phosducin knockout mice [45]. Another protein UNC 119 was suggested as well to help the light-driven translocation of transducin. In UNC 119 knockout mice, transducin α subunit partially remained in the inner segment and a significant slow return to the outer segment occurred upon dark adaptation [46]. However, the relationship between UNC 119 and transducin

βγ subunits has not been reported yet. It was demonstrated that centrin, a Ca^{2+}-binding protein located in the connecting cilium, might contribute to the transducin translocation as well due to its binding affinity to βγ subunits which therefore hindered transducin diffusion via the connecting cilium in the dark [53, 54]. Other binding partners such as Leu-Gly-Asn repeated-enriched protein (LGN) have also been proposed, but further investigation of their functions in transducin translocation are still needed [55, 56].

Alternative models were established for light-dependent transport of transducin. The mechanism of active transport with motor-driven machinery was proposed because the slow light-stimulated translocation of transducin to the inner segment was observed when exposed to microtubule-disrupting drugs [57]. However, the authors still failed to exclude the nonspecific effects of the microtubule poisons. In addition, the transducin movement should be disrupted by ATP deprivation if the transport depends on active transport. Researchers discovered that ATP deprivation did not lead to the impairment of transducin translocation from the inner segment to outer segment, however, disrupted the transducin movement from the outer segment to inner segment [44]. ATP is required for GTP synthesis, hence this impairment might be caused by the lack of GTP, which is important for transducin release from photoactivated rhodopsin. As expected, the group found that the transducin translocation from outer segment to inner segment was significantly impaired in GTP-depleted cells. Therefore, it was likely that the impairment of transducin movement caused by ATP depletion was because of the lack of GTP instead of ATP, further ruling out the possibility of the active transport mechanism.

In summary, the mechanism of transducin translocation is proposed to be diffusion with binding partner, however, how the heteotrimeric transducin complex could restore in the inner segment, and how they could dissociate from each other and return to the outer segment have not

been found yet. In addition, it is still unclear whether diffusion is sufficient to explain transducin return to its dark adapted status [16].

1.2.2 Light-Dependent Translocation of Recoverin

The light-driven translocation of recoverin follows the same direction as transducin [34-36]. The translocation of recoverin, a myristoylated Ca^{2+}-binding protein, can be explained by the diffusion hypothesis [58], although concrete mechanisms have not been explored yet [59]. A Ca^{2+}-myistoyl switch mechanism in recoverin was proposed, indicating that binding to Ca^{2+} led to the exposure of its myistoyl group and the enhancement of the binding affinity to membrane. Recoverin would freely move at low Ca^{2+} [59]. As a result, the final distribution of recoverin throughout the photoreceptor cells was determined by the membrane densities and the Ca^{2+} concentration [58]. Light absorption leads to the closure of cGMP-gated channels and the decrease of Ca^{2+} concentration in the outer segment, therefore, resulting in the reduced amount of recoverin in the outer segment upon light exposure. However, the explanation of recoverin's translocation into synaptic terminals is still obscure [16].

1.2.3 Light-Dependent Translocation of Arrestin

The first member of arrestin family was discovered as a soluble antigen related to the pathogenesis of experimental allergic uveitis (EAU) [60]. Hence, this protein was at first called S-antigen, encoded by SAG gene [61]. In addition, the self-association of S-antigen was indicated as well after purification [60]. Afterwards, a 48 kDa soluble protein was discovered, with the binding affinity to photoactivated phosphorylated rhodopsin [62] to suppress rhodopsin's capacity to activate transducin and cGMP phosphodiesterase [63]. Then the 48 kDa protein and S-antigen were considered as the same protein, named as "arrestin" due to its ability to "arrest" rhodopsin signaling[64].

Mammals express four arrestin subtypes [64, 65]. Among them, two subtypes in photoreceptors, rod (arrestin-1, visual arrestin) and cone (arrestin-4, X-arrestin) arrestin, have the ability to bind rhodopsin and cone opsins, respectively. The other two subtypes, arrestin-2 (β-arrestin) and arrestin-3 (β-arrestin2) are ubiquitously expressed and interact with hundreds of different GPCRs. The four arrestins all have an α-helix in the N-terminal domain and a polar core in C-terminal domain [66, 67] which could be disrupted on arrestin-receptor interaction [68]. In addition, the nonvisual arrestins have been demonstrated to have a clathrin-binding domain at the C-terminus [69]. Arrestin-4 is the only subtype that is a constitutive monomer [70], however, the other three subtypes have been shown to self-associate [64]. Among arrestin subtypes, rod arrestin is the only type that crystallized as a tetramer [67, 71, 72]. Its feature of robust self-association at physiological concentrations suggests its specific biological significance in rods [73]. Arrestin-2 and arrestin-3 are homologous adaptor proteins for GPCRs trafficking and signaling [68, 74-78], and self-association is regulated by IP6 (inositol 1,2,3,4,5,6-hexakisphosphate) [79], however, they form different oligomers. For instance, arrestin-2 forms large oligomers with the shape of long chains, and IP6 connects the N- and C-domains of adjacent molecules [79], while only dimers have been observed in arrestin-3 with the C-domains of two molecules connected by IP6 [64]. Therefore, the two nonvisual arrestins self-associate in their own ways, forming different types of oligomers. In contrast with the oligomerization of non-visual arrestins enhanced by IP6, the rod arrestin self-association is inhibited by IP6 [70].

In my study, I mainly focused on the visual arrestin. Light exposure led to massive translocation of phototransduction proteins between rod subcellular compartments. Among them, more than 90% of arrestin, which were responsible for quenching visual transduction [80], moved to the rod outer segment in response to light [16]. Such translocation of arrestin was

shown to be triggered in a critical threshold form [37]. Continuous light which bleached up to 1.5 % rhodopsin could not induce any discernible translocation of arrestin. However, doubling the light intensity (bleaching 3% rhodopsin) induced a significant arrestin translocation, and beyond this point, the relationship between the arrestin content in the rod outer segment and the amount of rhodopsin bleaching could be fitted by a straight line [37]. Strissel et al. also found that in dim light under the above circumstances, the amount of arrestin moved to outer segments was superstoichiometric to that of bleached rhodopsin, achieving the ratio of over 30-fold [37].

Although the phenomenon of light-driven arrestin translocation has been discovered for more than twenty years [34-36], the mechanism underlying this redistribution is still debatable. Several possible mechanisms were proposed in which arrestin translocated between rod subcellular compartments, including active transport [57, 81], diffusion with local binding partner [44, 82], diffusion barrier in ciliary transition zone [57, 83] and partitioning due to steric volume exclusion [84].

Some researchers supported the mechanism of active transport, because they believed that arrestin translocation needed ATP, which was an energy-dependent process [57, 81, 85, 86]; however, contrary results were reported that incubation of eyecups in the glucose-free media and supplemented with potassium cyanide and deoxyglucose, hence leading to the depletion of ATP, would disrupt the disruption of arrestin between rod compartments, which demonstrated that active transport was not able to be the mechanism of arrestin translocation in rod photoreceptors [44]. Besides, with the onset of illumination, ~3,000,000 arrestin translocated from the inner to the outer segment each minute [37], which was nearly 1000-fold faster than the motor-driven delivery of newly synthesized rhodopsin to the outer segment, a benchmark for the rapid motor driven protein transport process [16, 87]. The high speed of arrestin translocation was against the

active transport mechanism, unless arrestin moved in large aggregates or vesicles; but such structures were never detected [16], which crippled the possibility of active transport.

In bright light, arrestin is known to bind phosphorylated photoexcited rhodopsin in the outer segment [88], with the ratio of arrestin to rhodopsin at 1:1 [89], suggesting enough binding capacity in the outer segment. As a result, it is nature to consider that arrestin moves from the inner segment to outer segment by binding phosphorylated photoexcited rhodopsin and the binding sinks mechanism works. However, in dim light, people found the amount of arrestin translocating to the outer segment was superstoichiometric to the rhodopsin bleaching, with the ratio of 30:1, suggesting that there might not be enough binding sinks in the outer segment and the binding sinks mechanism did not work in dim light [17]. Peet et al [82] noticed that the intracellular distribution of arrestin in the dark was inconsistent with that of enhanced green fluorescent protein, which was a constitutive soluble protein. Several possible mechanisms could explain this phenomenon, and the first one was diffusion with binding partner in the inner segment. People have discovered three proteins that have associated with arrestin, including α-tubulin, enolase 1, and N-ethylmaleimide-sensitive factor (NSF). Microtubular cytoskeleton in the inner segment was one candidate for arrestin to bind, because arrestin had a low affinity for microtubules in the dark [44, 90, 91] and arrestin was shown to colocalize with the microtubular axoneme in *Xenopus* rods [81, 92]. Therefore, the mechanism underlying the light-stimulated arrestin translocation was proposed by a "competitive, two binding sinks" model, in which it could be explained in detail as a simple competition between low affinity microtubule sites in the inner segment and high affinity phosphorylated photoexcited rhodopsin sites in the outer segment [16, 44]. However, the expression level of α-tubulin was much lower than that of arrestin. The concentration of α-tubulin was only 50 μM in neural cells [93], while arrestin was

at millimolar levels [37]. With the low concentration at ~5 μM in rods [94], the other binding partner, enolase 1, was also ruled out. A third binding sites, NSF, was excluded as well due to the lack of co-localization with arrestin in rods [95]. As a result, the mechanism underlying the light-driven movement of arrestin from outer to inner segment might not be diffusion and binding with any local binding partners among microtubule, enolase 1 or NSF. Although it was believed that it was the free diffusion with binding to light-activated phosphorylated rhodopsin that probably led to arrestin movement from inner to outer segment, the low affinity to the proposed binding partners in the inner segment failed to sufficiently support the hypothesis of arrestin's moving back to the inner segment.

The mechanism of diffusion barrier was also studied. It was proposed that in the ciliary transition zone a diffusion barrier existed which stopped arrestin from moving to the outer segment without active transport machinery [57, 83]. However, researchers were not supportive of this hypothesis. Calvert et al [96] performed confocal and multiphoton microscopy experiments and tested the diffusion coefficient (D) of soluble photoactivatable green fluorescent protein (PAGFP) in the *Xenopus* connecting cilium (CC), rod inner segment (IS) and rod outer segment (OS), showing that D_{cc}=2.5 $\mu m^2 s^{-1}$ was only half of D_{IS} =5.2 $\mu m^2 s^{-1}$, and CC probably did not possess a diffusion barrier to arrestin movement which was a soluble protein as well, because PAGFP diffused much more rapidly in IS than any other compartments . In addition, Najafi et al stated that there were no significant differences between the fluxes of monomer and 3*PAGFP through the ciliary transition zone, suggesting that the ciliary transition zone could not contain a diffusion barrier and further weakened the mechanism of diffusion barrier [84].

In the same paper, Najafi et al also expressed GFP monomers, dimers and trimmers in *Xenopus* rod photoreceptors, and demonstrated that in the steady-state, the distribution patterns

of GFP oligomers were different [84]: compared with calcein, which was a small soluble protein, GFP monomers localized in the outer segment at 1.8-fold lower abundance when normalized to the amount in the inner segment, while the dimers and trimmers were shown at 2.9- and 6.8-fold, respectively. Hence, the altered crowding of the cytoplasm, which was due to cell structures and proteins, led to the distribution patterns of soluble proteins dependent on their shape and size via a mechanism named steric volume exclusion. They introduced such dynamic and size-dependent compartmental separation as the mechanism of soluble protein translocation, including arrestin, to rod outer segment. It has been known that self-association is a common property in visual arrestin at physiology concentrations [97], with the arrestin monomer size (48 kDa [98]) remarkably similar as that of GFP dimers (54 kDa for GFP dimer [99]). Thus, the mechanism underlying the light-stimulated translocation of arrestin was proposed to include the free diffusion to the outer segment through the connecting cilium with binding affinity to light-activated phosphorylated rhodopsin in the outer segment and travelling back to the inner segment was due to steric volume exclusion.

1.3. Self-Association of Visual Arrestin

1.3.1 Self-Association of Bovine, Mouse and Human Arrestin

The phenomenon of visual arrestin self-association was first discovered in 1977 by Wacker et al from analytical ultracentrifugation studies [60]. More recently, researchers conducted this subject and found that visual arrestin carried on a monomer-dimer equilibrium at physiological concentrations from sedimentation equilibrium experiment [100]. In addition, two groups performed Small Angle X-ray Scattering (SAXS) study and determined that the dominant species of bovine visual arrestin at physiological concentration (>1mM) [33, 37, 73, 89, 101] was

either dimers [102] or tetramers [103], with a monomer-dimer equilibrium or monomer-dimer-tetramer equilibrium, respectively.

Bovine, mouse and human arrestin have been shown to form dimers and tetramers with different self-association constants from multiangle light scattering experiment [97], among which, nocturnal mice that depend more on rod vision, obtain the highest concentration of monomer, while diurnal human beings that depend more on cone vision, get the lowest monomer concentration [3]. Kim et al. compared the self-association patterns of bovine, mouse and human visual arrestin and found that mouse and human arrestin self-associated, as well as bovine arrestin, with monomer-dimer-tetramer (MDT) equilibrium. However, the dimerization and tetramerization constants were different among these species, with $K_{D,dim}$ (37.2 μM)>$K_{D,tet}$ (7.4 μM) in bovine arrestin, $K_{D,dim}$ (57.5 μM)~$K_{D,tet}$ (63.1 μM) in mouse arrestin, and $K_{D,dim}$ (2.95 μM)<<$K_{D,tet}$ (224 μM) in human arrestin [97]. The authors also calculated by the MDT model and found the relationship between the percentage of mouse or human arrestin in monomer, dimer or tetramer forms and arrestin concentration. According to their data, arrestin was predicted to be oligomers at high concentrations of arrestin in all three species, however, arrestin remained as monomers at low concentrations of arrestin (Fig.5).

Arrestin self-association is conserved in mouse, bovine and humans [97], which suggests that it should contain a certain biological function. It was suggested that the oligomerization of arrestin enabled rods to possess huge supply of arrestin in bright light and maintain monomer concentration at a relatively low level in the dark [3]. Only arrestin monomer is able to bind to photoexcited phosphorylated rhodopsin, therefore, oligomers are likely to serve as a storage form of arrestin and is readily to dissociate in order to provide active monomer when preventing rhodopsin signaling [73]. The active rhodopsin lifetime is very short, and because the dimer

dissociation might lead to a delay which rods could not afford, rod photoreceptors should have an arrestin monomer concentration high enough for rhodopsin binding without any delay [73]. Physiological expression of arrestin in rod photoreceptors represents a balance between functional performance and long-term protection of photoreceptor cells [104]. In humans, genetic mutations lead to the deficiency of arrestin and its improper transport, resulting in the problems of stationary night blindness, prolonged activation of rhodopsin and rod degeneration [105]. Bovine, mouse and human arrestin can form soluble dimers and tetramers at physiological concentrations. Therefore, arrestin distribution may be governed by the size of arrestin oligomers and regulated by oligomerization. As a result, the mechanism of steric volume exclusion might be able to answer the question of how arrestin was effectively excluded from the outer segments of dark-adapted rods [84].

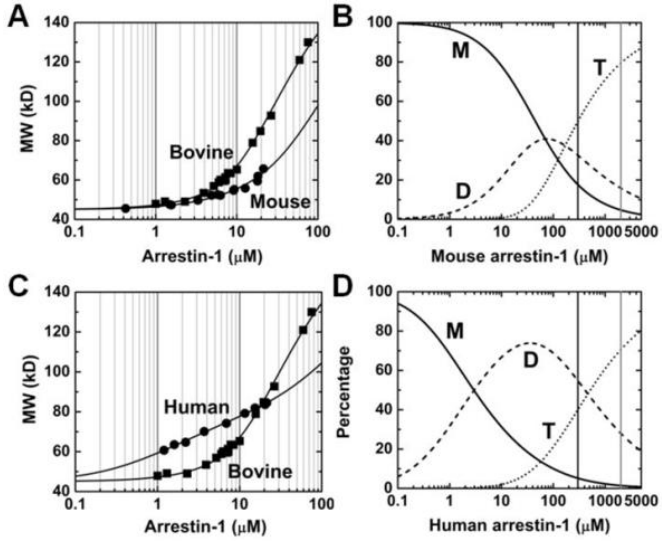

Figure 5 Bovine, mouse and human arrestin-1 form dimers and tetramers at physiological concentrations. A and C. The average molecular weight of wild type bovine, mouse, or human arrestin as a function of total concentration (black circles), respectively. B and D. The percentage of mouse or human arrestin molecules in monomer (M, straight line), dimer (D, dashed line), and tetramer (T, dotted line) as a function of total arrestin concentration, respectively[97].

The structures of the crystal (Fig.6A, [65, 73]) and proposed solution (Fig.6B, [97]) tetramers were shown different from the electron paramagnetic resonance (EPR) experiments [73]. Crystal tetramer structure contained two interfaces: a CN interface which was the C domain of one arrestin with the N domain of another; and a CC interface which was two C domains [73]. Another interface was between tetramers, which was an NN interface. Proposed tetramer structure in solution had two interfaces: a CC interface which was between two C domains; and an NN interface which was between two N domains [97]. Residues of I72, F79, L173, T233 and V244, which were not at any contacts in crystal structure, were presented at the tetramer interface in solution, suggesting that the crystal structure was not the same as solution structure.

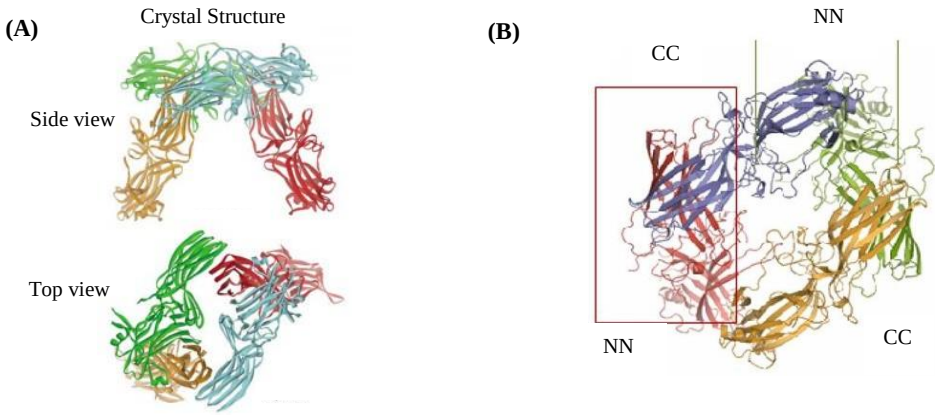

Figure 6 The crystal (A) [73] and solution (B) [97] structures of visual arrestin tetramer.

Several residues in bovine arrestin which were proposed crucial for arrestin oligomerization, were determined and self-association was shown to be disrupted when replacing these residues with alanines [65, 73, 97]. Based on the bovine arrestin construct, Kim et al. introduced two mutations (F85A, F197A) which led to the disruption of NN (F85A) and CC (F197A) interfaces, and it was proved to disrupt the oligomerization of bovine arrestin at some extent, with $K_{D,dim}$ increased from 37.2 μM to 525 μM and no detectable tetramer formation [97].

This high dissociation constant value demonstrated that arrestin would be essentially monomeric form at lower concentrations, but would still dimerize at higher concentrations in physiological concentration range. According to the light scattering and electron paramagnetic resonance (EPR) data, bovine phenylalanine residue 79, which was located in the CN self-association interface in crystal structure, was also involved in intersubunit interactions of arrestin tetramer in solution [73]. Similar mutations in mouse arrestin also resulted in essentially monomeric form *in vitro* [97], showing that these residues were conserved interacting regions for arrestin oligomerization [73]. Homologous mutations (F86A, F198A) were introduced in mouse arrestin with similar phenomenon of disrupting arrestin oligomerization as bovine arrestin (2A). The dimer dissociation constant was shown 537 μM with no detectable tetramer formation [97]. However, these mutations did not affect the binding affinity to either light-activated phosphorylated rhodopsin or microtubules, indicating that the mutations only disrupted the self-association interfaces instead of leading to global conformational changes [97], otherwise, the binding affinities would be significantly affected even when small structural perturbations happened [22, 91, 106-113]. These residues are shown to be conserved in mammalian visual arrestin [114] and self-association is a common feature in mammalian visual arrestin [3, 97].

1.3.2 Self-Association of Xenopus Arrestin

Xenopus laevis are used as the experimental model in retinal studies due to their large rod photoreceptor outer segments with the diameter of approximately 7 μm [115-117]. Together with other advantages, such as rapid eye development, generating large amount of eggs in one day, and easy manipulation of experiments because embryonic development is outside the mother [116], etc., *Xenopus laevis* are regarded as the favorite experimental model which have been widely used since 1970s by Papermaster's group to explore the polarized protein trafficking of

opsin [118-120]. In previous work, our laboratory has also established the *Xenopus* rod photoreceptors as an incomparable experimental model system, for testing how the interplay of cell structures and proteins of different molecular sizes and shapes influenced cell activities [84].

As shown in Fig.6, bovine and *Xenopus* arrestins share 70% similarity by using the BLAST function on NCBI website, and *Xenopus* residues F78, Y84 and F193 are analogous to bovine residues F79, F85 and F197 by using the alignment function of Lasergene's Pro MegAlign software (or BLAST function on NCBI website). As a result, we predict that *Xenopus* arrestin F78, Y84 and F193 are also important for arrestin oligomerization. Although mouse, bovine, and human arrestin have been shown to form dimers and tetramers at a concentration dependent manner, the oligomeric form of *Xenopus* has never been reported [97]. Hence, my work will be the first time to present the oligomeric state of *Xenopus* arrestin.

Figure 6 Bovine and *Xenopus* arrestin have 70% similarity. Bovine F79, F85 and F197 corresponds to *Xenopus* F78 (black shadow), Y84 (red circle) and F193 (purple square), respectively.

1.4. Clinical Significance

The enhanced arrestin mutant, 3A, which significantly increased the binding to unphosphorylated photoexcited rhodopsin compared with wild-type arrestin, was transgenically expressed in mice [106]. The authors found that in mice with phosphorylated rhodopsin, wild-type arrestin had healthier retinal photoreceptors than mutant; however, in mice lacking rhodopsin kinase, the enhanced arrestin mutant protected photoreceptor health significantly, compared with the wild-type arrestin. Defects in rhodopsin termination leads to several visual disorders, including Oguchi disease, which is a stationary night blindness [121, 122]. Oguchi disease, which causes reduced visual acuity and decreased visual fields, was originally

discovered in Japan, and subsequently also found in American, Pakistani, Indian and European patients. Although rod functions were reduced, electroretinography presented normal cone functions [123, 124]. The disease is an autosomal recessive inherited disease [121], which was shown to be caused by mutations in arrestin gene and rhodopsin kinase gene [125]. As a result, the introduction of the enhanced arrestin to shut off signaling cascade is one of the strategies for gene therapy, which improves the recovery performance, promotes rod photoreceptor survival, and smoothes the way for the compensational gene therapy development for congenital disorders [3].

Many genetic mutations, which lead to blindness, deafness, mental retardation, kidney disease and other related maladies, result from the improper transport and localization of proteins to sensory and primary cilia. Retinitis Pigmentosa (RP), which is the most common human retinopathy of genetic origin [126], is a group of disorders in which aberrations of rods and cones result in progressive visual loss. At first, patients underwent impaired dark adaptation or night blindness, which was followed by visual fields constriction and ultimately vision loss [127]. Hence, the determination of light-dependent translocation of phototransduction proteins in the rod subcellular compartments supplies the evidence for the discovery of blindness causes and the basis for new cures [128]. Understanding the mechanisms that underlie arrestin transport in photoreceptors might lead to therapeutic methods to slow and even cure photoreceptor degeneration. Diseases that are caused by defective arrestin oligomerization might be alleviated by designing drugs that could change improper arrestin translocation and distribution. In addition, the transport of proteins through cilia is important for cell survival, and the transport impairment could lead to cell degeneration and diseases such as tumor [96]. Although arrestin has been studied for decades, many important aspects still remain to be clarified. The biological

role of the robust self-association and oligomerization among several species still need to be clearly elucidated. Moreover, the exact light-dependent arrestin translocation mechanism and whether there is a relationship between arrestin oligomerization and translocation need to be determined as well, which might pave the way for the therapeutic development of molecular tools [3].

1.5 Objectives and dissertation outline

The main objective of my work is to provide an integrated understanding of the self-association phenomenon in bovine, mouse and *Xenopus* arrestin in solution. This understanding is critical, because it could lay the foundation for the proposed mechanism "steric volume exclusion", which might be able to explain how visual arrestin is excluded from the rod outer segments in dark-adapted state. The oligomerization formation of wild-type bovine, mouse and *Xenopus* arrestin was investigated and their equilibrium constants were calculated. Moreover, *Xenopus* arrestin with mutations was also studied to explore whether the residues which were proposed to disrupt the self-association interfaces, could also be reserved in *Xenopus* arrestin.

Chapter 2 studied the oligomerization phenomenon of bovine, mouse and *Xenopus* wild-type arrestin, and *Xenopus* arrestin with mutations. The proteins were expressed in *E.coli* and purified by hexa-his tag affinity to Nickel-Agarose [129]. Analytical ultracentrifugation experiments were performed to determine the concentration-dependent tendency to form oligomers of the proteins.

Chapter 3 summarized the topics in my study. It also discussed the significance of my work and the future directions of the study.

Reference

1. Wassle, H., *Parallel processing in the mammalian retina.* Nat Rev Neurosci, 2004. **5**(10): p. 747-57.
2. Slepak, V.Z. and J.B. Hurley, *Mechanism of light-induced translocation of arrestin and transducin in photoreceptors: interaction-restricted diffusion.* IUBMB Life, 2008. **60**(1): p. 2-9.
3. Gurevich, V.V., et al., *The functional cycle of visual arrestins in photoreceptor cells.* Prog Retin Eye Res, 2011. **30**(6): p. 405-30.
4. Mustafi, D., A.H. Engel, and K. Palczewski, *Structure of cone photoreceptors.* Prog Retin Eye Res, 2009. **28**(4): p. 289-302.
5. Peters, K.R., et al., *Fine structure of a periciliary ridge complex of frog retinal rod cells revealed by ultrahigh resolution scanning electron microscopy.* J Cell Biol, 1983. **96**(1): p. 265-76.
6. Corless, J.M. and T.G. Schneider, *Patterns of interdisk connections within the lamellar domains of retinal rod outer segment disks: observations relevant to the axial propagation of incisures.* Exp Eye Res, 1987. **45**(6): p. 883-905.
7. Nickell, S., et al., *Three-dimensional architecture of murine rod outer segments determined by cryoelectron tomography.* J Cell Biol, 2007. **177**(5): p. 917-25.
8. Albert, A.D. and K. Boesze-Battaglia, *The role of cholesterol in rod outer segment membranes.* Prog Lipid Res, 2005. **44**(2-3): p. 99-124.
9. Townes-Anderson, E., P.R. MacLeish, and E. Raviola, *Rod cells dissociated from mature salamander retina: ultrastructure and uptake of horseradish peroxidase.* J Cell Biol, 1985. **100**(1): p. 175-88.
10. Young, R.W. and B. Droz, *The renewal of protein in retinal rods and cones.* J Cell Biol, 1968. **39**(1): p. 169-84.
11. Anderson, D.H. and S.K. Fisher, *The photoreceptors of diurnal squirrels: outer segment structure, disc shedding, and protein renewal.* J Ultrastruct Res, 1976. **55**(1): p. 119-41.
12. Toyoda, J., et al., *The rod response in the frog and studies by intracellular recording.* Vision Res, 1970. **10**(11): p. 1093-100.
13. Baylor, D.A., *Photoreceptor signals and vision. Proctor lecture.* Invest Ophthalmol Vis Sci, 1987. **28**(1): p. 34-49.
14. Molday, R.S., R. Warren, and T.S. Kim, *Purification and biochemical analysis of cGMP-gated channel and Na+/Ca(2+)-K+ exchanger of rod photoreceptors.* Methods Enzymol, 2000. **315**: p. 831-47.
15. Pugh Jr, E.N. and T.D. Lamb, *Phototransduction in vertebrate rods and cones: Molecular mechanisms of amplification, recovery and light adaptation.* Handbook of Biological Physics. Molecular Mechanisms in Visual Transduction, 2000. **3**: p. 183-255.
16. Calvert, P.D., et al., *Light-driven translocation of signaling proteins in vertebrate photoreceptors.* Trends in Cell Biology, 2006. **16**(11): p. 560-568.
17. Sokolov, M., et al., *Massive Light-Driven Translocation of Transducin between the Two Major Compartments of Rod Cells: A Novel Mechanism of Light Adaptation.* Neuron, 2002. **34**(1): p. 95-106.
18. Govardovskii, V.I., P.D. Calvert, and V.Y. Arshavsky, *Photoreceptor light adaptation. Untangling desensitization and sensitization.* J Gen Physiol, 2000. **116**(6): p. 791-4.
19. Berridge, M.J., P. Lipp, and M.D. Bootman, *The versatility and universality of calcium signalling.* Nat Rev Mol Cell Biol, 2000. **1**(1): p. 11-21.
20. Krizaj, D. and D.R. Copenhagen, *Calcium regulation in photoreceptors.* Front Biosci, 2002. **7**: p. d2023-44.
21. Korenbrot, J.I. and T.I. Rebrik, *Tuning outer segment Ca2+ homeostasis to phototransduction in rods and cones.* Adv Exp Med Biol, 2002. **514**: p. 179-203.

22. Gray-Keller, M.P., et al., *Arrestin with a single amino acid substitution quenches light-activated rhodopsin in a phosphorylation-independent fashion.* Biochemistry, 1997. **36**(23): p. 7058-63.
23. Berg, J.M., J.L. Tymoczko, and L. Stryer, *Biochemistry, ; W. H*. 2002, Freeman and Company: New York.
24. Olshevskaya, E., A. Ermilov, and A. Dizhoor, *Factors that affect regulation of cGMP synthesis in vertebrate photoreceptors and their genetic link to human retinal degeneration.* Molecular and Cellular Biochemistry, 2002. **230**(1-2): p. 139-147.
25. Sampath, A.P., et al., *Light-dependent changes in outer segment free-Ca2+ concentration in salamander cone photoreceptors.* J Gen Physiol, 1999. **113**(2): p. 267-77.
26. Hodgkin, A.L. and B.J. Nunn, *Control of light-sensitive current in salamander rods.* J Physiol, 1988. **403**: p. 439-71.
27. Kawamura, S., *Rhodopsin phosphorylation as a mechanism of cyclic GMP phosphodiesterase regulation by S-modulin.* Nature, 1993. **362**(6423): p. 855-7.
28. Hackos, D.H. and J.I. Korenbrot, *Calcium modulation of ligand affinity in the cyclic GMP-gated ion channels of cone photoreceptors.* J Gen Physiol, 1997. **110**(5): p. 515-28.
29. Hsu, Y.T. and R.S. Molday, *Modulation of the cGMP-gated channel of rod photoreceptor cells by calmodulin.* Nature, 1993. **361**(6407): p. 76-9.
30. Li, N., et al., *Identification of functional regions of guanylate cyclase-activating protein 1 (GCAP1) using GCAP1/GCIP chimeras.* Biol Chem, 2001. **382**(8): p. 1179-88.
31. Rebrik, T.I., E.A. Kotelnikova, and J.I. Korenbrot, *Time course and Ca(2+) dependence of sensitivity modulation in cyclic GMP-gated currents of intact cone photoreceptors.* J Gen Physiol, 2000. **116**(4): p. 521-34.
32. Chen, C.K., et al., *Ca(2+)-dependent interaction of recoverin with rhodopsin kinase.* J Biol Chem, 1995. **270**(30): p. 18060-6.
33. Broekhuyse, R.M., et al., *Light induced shift and binding of S-antigen in retinal rods.* Curr Eye Res, 1985. **4**(5): p. 613-8.
34. Philp, N.J., W. Chang, and K. Long, *Light-stimulated protein movement in rod photoreceptor cells of the rat retina.* FEBS Lett, 1987. **225**(1-2): p. 127-32.
35. Whelan, J.P. and J.F. McGinnis, *Light-dependent subcellular movement of photoreceptor proteins.* J Neurosci Res, 1988. **20**(2): p. 263-70.
36. Brann, M.R. and L.V. Cohen, *Diurnal expression of transducin mRNA and translocation of transducin in rods of rat retina.* Science, 1987. **235**(4788): p. 585-7.
37. Strissel, K.J., et al., *Arrestin translocation is induced at a critical threshold of visual signaling and is superstoichiometric to bleached rhodopsin.* J Neurosci, 2006. **26**(4): p. 1146-53.
38. Palczewski, K., *Structure and functions of arrestins.* Protein Sci, 1994. **3**(9): p. 1355-61.
39. Chan, S., et al., *Functional comparisons of visual arrestins in rod photoreceptors of transgenic mice.* Invest Ophthalmol Vis Sci, 2007. **48**(5): p. 1968-75.
40. Xu, J., et al., *Prolonged photoresponses in transgenic mouse rods lacking arrestin.* Nature, 1997. **389**(6650): p. 505-9.
41. Arshavsky, V.Y., *Protein translocation in photoreceptor light adaptation: a common theme in vertebrate and invertebrate vision.* Sci STKE, 2003. **2003**(204): p. PE43.
42. Kassai, H., et al., *Farnesylation of retinal transducin underlies its translocation during light adaptation.* Neuron, 2005. **47**(4): p. 529-39.
43. Elias, R.V., et al., *Temporal kinetics of the light/dark translocation and compartmentation of arrestin and alpha-transducin in mouse photoreceptor cells.* Mol Vis, 2004. **10**: p. 672-81.
44. Nair, K.S., et al., *Light-Dependent Redistribution of Arrestin in Vertebrate Rods Is an Energy-Independent Process Governed by Protein-Protein Interactions.* Neuron, 2005. **46**(4): p. 555-567.

45. Sokolov, M., et al., *Phosducin facilitates light-driven transducin translocation in rod photoreceptors. Evidence from the phosducin knockout mouse.* J Biol Chem, 2004. **279**(18): p. 19149-56.
46. Zhang, H., et al., *UNC119 is required for G protein trafficking in sensory neurons.* Nat Neurosci, 2011. **14**(7): p. 874-80.
47. Kerov, V., et al., *Transducin activation state controls its light-dependent translocation in rod photoreceptors.* J Biol Chem, 2005. **280**(49): p. 41069-76.
48. He, W., C.W. Cowan, and T.G. Wensel, *RGS9, a GTPase accelerator for phototransduction.* Neuron, 1998. **20**(1): p. 95-102.
49. Lobanova, E.S., et al., *Transducin translocation in rods is triggered by saturation of the GTPase-activating complex.* J Neurosci, 2007. **27**(5): p. 1151-60.
50. Rosenzweig, D.H., et al., *Subunit dissociation and diffusion determine the subcellular localization of rod and cone transducins.* J Neurosci, 2007. **27**(20): p. 5484-94.
51. Gaudet, R., A. Bohm, and P.B. Sigler, *Crystal structure at 2.4 angstroms resolution of the complex of transducin betagamma and its regulator, phosducin.* Cell, 1996. **87**(3): p. 577-88.
52. Murray, D., S. McLaughlin, and B. Honig, *The role of electrostatic interactions in the regulation of the membrane association of G protein beta gamma heterodimers.* J Biol Chem, 2001. **276**(48): p. 45153-9.
53. Pulvermuller, A., et al., *Calcium-dependent assembly of centrin-G-protein complex in photoreceptor cells.* Mol Cell Biol, 2002. **22**(7): p. 2194-203.
54. Giessl, A., et al., *Differential expression and interaction with the visual G-protein transducin of centrin isoforms in mammalian photoreceptor cells.* J Biol Chem, 2004. **279**(49): p. 51472-81.
55. Nair, K.S., et al., *The presence of a Leu-Gly-Asn repeat-enriched protein (LGN), a putative binding partner of transducin, in ROD photoreceptors.* Invest Ophthalmol Vis Sci, 2005. **46**(1): p. 383-9.
56. Kerov, V.S., M. Natochin, and N.O. Artemyev, *Interaction of transducin-alpha with LGN, a G-protein modulator expressed in photoreceptor cells.* Mol Cell Neurosci, 2005. **28**(3): p. 485-95.
57. Peterson, J.J., et al., *A role for cytoskeletal elements in the light-driven translocation of proteins in rod photoreceptors.* Invest Ophthalmol Vis Sci, 2005. **46**(11): p. 3988-98.
58. Strissel, K.J., et al., *Recoverin undergoes light-dependent intracellular translocation in rod photoreceptors.* J Biol Chem, 2005. **280**(32): p. 29250-5.
59. Ames, J.B., et al., *Portrait of a myristoyl switch protein.* Curr Opin Struct Biol, 1996. **6**(4): p. 432-8.
60. Wacker, W.B., et al., *Experimental allergic uveitis. Isolation, characterization, and localization of a soluble uveitopathogenic antigen from bovine retina.* J Immunol, 1977. **119**(6): p. 1949-58.
61. Yamaki, K., et al., *Structural organization of the human S-antigen gene. cDNA, amino acid, intron, exon, promoter, in vitro transcription, retina, and pineal gland.* J Biol Chem, 1990. **265**(34): p. 20757-62.
62. Kuhn, H., S.W. Hall, and U. Wilden, *Light-induced binding of 48-kDa protein to photoreceptor membranes is highly enhanced by phosphorylation of rhodopsin.* FEBS Lett, 1984. **176**(2): p. 473-8.
63. Wilden, U., S.W. Hall, and H. Kuhn, *Phosphodiesterase activation by photoexcited rhodopsin is quenched when rhodopsin is phosphorylated and binds the intrinsic 48-kDa protein of rod outer segments.* Proc Natl Acad Sci U S A, 1986. **83**(5): p. 1174-8.
64. Chen, Q., et al., *Self-association of arrestin family members.* Handb Exp Pharmacol, 2014. **219**: p. 205-23.
65. Hanson, S.M., et al., *A model for the solution structure of the rod arrestin tetramer.* Structure, 2008. **16**(6): p. 924-34.
66. Gurevich, V.V. and E.V. Gurevich, *The molecular acrobatics of arrestin activation.* Trends Pharmacol Sci, 2004. **25**(2): p. 105-11.

67. Hirsch, J.A., et al., *A Model for Arrestin's Regulation: The 2.8 Å Crystal Structure of Visual Arrestin.* Cell, 1999. **97**(2): p. 257-269.
68. Han, S.O., R.P. Kommaddi, and S.K. Shenoy, *Distinct roles for beta-arrestin2 and arrestin-domain-containing proteins in beta2 adrenergic receptor trafficking.* EMBO Rep, 2013. **14**(2): p. 164-71.
69. Krupnick, J.G., et al., *Arrestin/clathrin interaction. Localization of the clathrin binding domain of nonvisual arrestins to the carboxy terminus.* J Biol Chem, 1997. **272**(23): p. 15011-6.
70. Hanson, S.M., et al., *Opposing effects of inositol hexakisphosphate on rod arrestin and arrestin2 self-association.* Biochemistry, 2008. **47**(3): p. 1070-5.
71. Han, M., et al., *Crystal structure of beta-arrestin at 1.9 A: possible mechanism of receptor binding and membrane Translocation.* Structure, 2001. **9**(9): p. 869-80.
72. Sutton, R.B., et al., *Crystal structure of cone arrestin at 2.3A: evolution of receptor specificity.* J Mol Biol, 2005. **354**(5): p. 1069-80.
73. Hanson, S.M., et al., *Structure and function of the visual arrestin oligomer.* EMBO J, 2007. **26**(6): p. 1726-36.
74. Shenoy, S.K., et al., *Regulation of receptor fate by ubiquitination of activated beta 2-adrenergic receptor and beta-arrestin.* Science, 2001. **294**(5545): p. 1307-13.
75. Shenoy, S.K., et al., *Nedd4 mediates agonist-dependent ubiquitination, lysosomal targeting, and degradation of the beta2-adrenergic receptor.* J Biol Chem, 2008. **283**(32): p. 22166-76.
76. Bhandari, D., et al., *Arrestin-2 interacts with the ubiquitin-protein isopeptide ligase atrophin-interacting protein 4 and mediates endosomal sorting of the chemokine receptor CXCR4.* J Biol Chem, 2007. **282**(51): p. 36971-9.
77. Shukla, A.K., et al., *Arresting a transient receptor potential (TRP) channel: beta-arrestin 1 mediates ubiquitination and functional down-regulation of TRPV4.* J Biol Chem, 2010. **285**(39): p. 30115-25.
78. Simonin, A. and D. Fuster, *Nedd4-1 and beta-arrestin-1 are key regulators of Na+/H+ exchanger 1 ubiquitylation, endocytosis, and function.* J Biol Chem, 2010. **285**(49): p. 38293-303.
79. Xu, T.R., et al., *Mutations of beta-arrestin 2 that limit self-association also interfere with interactions with the beta2-adrenoceptor and the ERK1/2 MAPKs: implications for beta2-adrenoceptor signalling via the ERK1/2 MAPKs.* Biochem J, 2008. **413**(1): p. 51-60.
80. Krupnick, J.G., V.V. Gurevich, and J.L. Benovic, *Mechanism of quenching of phototransduction. Binding competition between arrestin and transducin for phosphorhodopsin.* J Biol Chem, 1997. **272**(29): p. 18125-31.
81. McGinnis, J.F., et al., *Cytoskeleton participation in subcellular trafficking of signal transduction proteins in rod photoreceptor cells.* J Neurosci Res, 2002. **67**(3): p. 290-7.
82. Peet, J.A., et al., *Quantification of the cytoplasmic spaces of living cells with EGFP reveals arrestin-EGFP to be in disequilibrium in dark adapted rod photoreceptors.* J Cell Sci, 2004. **117**(Pt 14): p. 3049-59.
83. Marszalek, J.R., et al., *Genetic Evidence for Selective Transport of Opsin and Arrestin by Kinesin-II in Mammalian Photoreceptors.* Cell, 2000. **102**(2): p. 175-187.
84. Najafi, M., N.A. Maza, and P.D. Calvert, *Steric volume exclusion sets soluble protein concentrations in photoreceptor sensory cilia.* Proc Natl Acad Sci U S A, 2012. **109**(1): p. 203-8.
85. Orisme, W., et al., *Light-dependent translocation of arrestin in rod photoreceptors is signaled through a phospholipase C cascade and requires ATP.* Cell Signal, 2010. **22**(3): p. 447-56.
86. Reidel, B., et al., *The translocation of signaling molecules in dark adapting mammalian rod photoreceptor cells is dependent on the cytoskeleton.* Cell Motil Cytoskeleton, 2008. **65**(10): p. 785-800.

87. Liu, X., et al., *Myosin VIIa participates in opsin transport through the photoreceptor cilium.* J Neurosci, 1999. **19**(15): p. 6267-74.
88. Mangini, N.J., et al., *Effect of hydroxylamine on the subcellular distribution of arrestin (S-antigen) in rod photoreceptors.* Vis Neurosci, 1994. **11**(3): p. 561-8.
89. Hanson, S.M., et al., *Each rhodopsin molecule binds its own arrestin.* Proc Natl Acad Sci U S A, 2007. **104**(9): p. 3125-8.
90. Nair, K.S., et al., *Direct binding of visual arrestin to microtubules determines the differential subcellular localization of its splice variants in rod photoreceptors.* J Biol Chem, 2004. **279**(39): p. 41240-8.
91. Hanson, S.M., et al., *Visual arrestin binding to microtubules involves a distinct conformational change.* J Biol Chem, 2006. **281**(14): p. 9765-72.
92. Peterson, J.J., et al., *Arrestin migrates in photoreceptors in response to light: a study of arrestin localization using an arrestin-GFP fusion protein in transgenic frogs.* Experimental Eye Research, 2003. **76**(5): p. 553-563.
93. Hiller, G. and K. Weber, *Radioimmunoassay for tubulin: a quantitative comparison of the tubulin content of different established tissue culture cells and tissues.* Cell, 1978. **14**(4): p. 795-804.
94. Smith, W.C., et al., *Interaction of arrestin with enolase1 in photoreceptors.* Invest Ophthalmol Vis Sci, 2011. **52**(3): p. 1832-40.
95. Huang, S.P., B.M. Brown, and C.M. Craft, *Visual Arrestin 1 acts as a modulator for N-ethylmaleimide-sensitive factor in the photoreceptor synapse.* J Neurosci, 2010. **30**(28): p. 9381-91.
96. Calvert, P.D., W.E. Schiesser, and E.N. Pugh, Jr., *Diffusion of a soluble protein, photoactivatable GFP, through a sensory cilium.* J Gen Physiol, 2010. **135**(3): p. 173-96.
97. Kim, M., et al., *Robust self-association is a common feature of mammalian visual arrestin-1.* Biochemistry, 2011. **50**(12): p. 2235-42.
98. Shinohara, T., et al., *Primary and secondary structure of bovine retinal S antigen (48-kDa protein).* Proc Natl Acad Sci U S A, 1987. **84**(20): p. 6975-9.
99. Hink, M.A., et al., *Structural dynamics of green fluorescent protein alone and fused with a single chain Fv protein.* J Biol Chem, 2000. **275**(23): p. 17556-60.
100. Schubert, C., et al., *Visual arrestin activity may be regulated by self-association.* J Biol Chem, 1999. **274**(30): p. 21186-90.
101. Hamm, H.E. and M.D. Bownds, *Protein complement of rod outer segments of frog retina.* Biochemistry, 1986. **25**(16): p. 4512-23.
102. Shilton, B.H., et al., *The solution structure and activation of visual arrestin studied by small-angle X-ray scattering.* Eur J Biochem, 2002. **269**(15): p. 3801-9.
103. Imamoto, Y., et al., *Concentration-Dependent Tetramerization of Bovine Visual Arrestin.* Biophysical Journal, 2003. **85**(2): p. 1186-1195.
104. Song, X., et al., *Arrestin-1 expression level in rods: balancing functional performance and photoreceptor health.* Neuroscience, 2011. **174**(0): p. 37-49.
105. Sommer, M.E. and D.L. Farrens, *Arrestin can act as a regulator of rhodopsin photochemistry.* Vision Res, 2006. **46**(27): p. 4532-46.
106. Song, X., et al., *Enhanced arrestin facilitates recovery and protects rods lacking rhodopsin phosphorylation.* Curr Biol, 2009. **19**(8): p. 700-5.
107. Gurevich, V.V., *The selectivity of visual arrestin for light-activated phosphorhodopsin is controlled by multiple nonredundant mechanisms.* J Biol Chem, 1998. **273**(25): p. 15501-6.
108. Hanson, S.M. and V.V. Gurevich, *The differential engagement of arrestin surface charges by the various functional forms of the receptor.* J Biol Chem, 2006. **281**(6): p. 3458-62.

109. Gurevich, V.V. and J.L. Benovic, *Visual arrestin binding to rhodopsin. Diverse functional roles of positively charged residues within the phosphorylation-recognition region of arrestin.* J Biol Chem, 1995. **270**(11): p. 6010-6.
110. Gurevich, V.V. and J.L. Benovic, *Mechanism of phosphorylation-recognition by visual arrestin and the transition of arrestin into a high affinity binding state.* Mol Pharmacol, 1997. **51**(1): p. 161-9.
111. Vishnivetskiy, S.A., et al., *How does arrestin respond to the phosphorylated state of rhodopsin?* J Biol Chem, 1999. **274**(17): p. 11451-4.
112. Vishnivetskiy, S.A., et al., *An additional phosphate-binding element in arrestin molecule. Implications for the mechanism of arrestin activation.* J Biol Chem, 2000. **275**(52): p. 41049-57.
113. Hanson, S.M., et al., *Arrestin mobilizes signaling proteins to the cytoskeleton and redirects their activity.* J Mol Biol, 2007. **368**(2): p. 375-87.
114. Gurevich, E.V. and V.V. Gurevich, *Arrestins: ubiquitous regulators of cellular signaling pathways.* Genome Biol, 2006. **7**(9): p. 236.
115. Xiong, W.H. and K.W. Yau, *Rod sensitivity during Xenopus development.* J Gen Physiol, 2002. **120**(6): p. 817-27.
116. Moritz, O.L., et al., *Fluorescent photoreceptors of transgenic Xenopus laevis imaged in vivo by two microscopy techniques.* Invest Ophthalmol Vis Sci, 1999. **40**(13): p. 3276-80.
117. Haeri, M., B.E. Knox, and A. Ahmadi, *Modeling the flexural rigidity of rod photoreceptors.* Biophys J, 2013. **104**(2): p. 300-12.
118. Papermaster, D.S. and W.J. Dreyer, *Rhodopsin content in the outer segment membranes of bovine and frog retinal rods.* Biochemistry, 1974. **13**(11): p. 2438-44.
119. Papermaster, D.S., C.A. Converse, and J. Siuss, *Membrane biosynthesis in the frog retina: opsin transport in the photoreceptor cell.* Biochemistry, 1975. **14**(7): p. 1343-52.
120. Papermaster, D.S., et al., *Immunocytochemical localization of a large intrinsic membrane protein to the incisures and margins of frog rod outer segment disks.* J Cell Biol, 1978. **78**(2): p. 415-25.
121. Fuchs, S., et al., *A homozygous 1-base pair deletion in the arrestin gene is a frequent cause of Oguchi disease in Japanese.* Nat Genet, 1995. **10**(3): p. 360-2.
122. Yamamoto, S., et al., *Defects in the rhodopsin kinase gene in the Oguchi form of stationary night blindness.* Nat Genet, 1997. **15**(2): p. 175-8.
123. Carr, R.E. and P. Gouras, *OGUCHI'S DISEASE.* Arch Ophthalmol, 1965. **73**: p. 646-56.
124. Miyake, Y., et al., *Electrophysiological findings in patients with Oguchi's disease.* Jpn J Ophthalmol, 1996. **40**(4): p. 511-9.
125. Huang, L., et al., *A Chinese family with Oguchi's disease due to compound heterozygosity including a novel deletion in the arrestin gene.* Mol Vis, 2012. **18**: p. 528-36.
126. Farrar, G.J., et al., *Autosomal dominant retinitis pigmentosa: linkage to rhodopsin and evidence for genetic heterogeneity.* Genomics, 1990. **8**(1): p. 35-40.
127. Fahim AT, D.S., Weleber RG, *Retinitis Pigmentosa Overviewji.* GeneReviews™ [Internet], 1993.
128. Vishnivetskiy, S.A., et al., *Engineering visual arrestin-1 with special functional characteristics.* J Biol Chem, 2013. **288**(5): p. 3394-405.
129. Gurevich, V.V. and J.L. Benovic, *Arrestin: mutagenesis, expression, purification, and functional characterization.* Methods Enzymol, 2000. **315**: p. 422-37.

CHAPTER 2 DETERMINATION OF BOVINE, MOUSE AND *XENOPUS* VISUAL ARRESTIN OLIGOMERIZATION

Work within this chapter is related to the manuscript in preparation:

Shuang Qiu, Stephen Shinsky, Michael Cosgrove, Peter Calvert*. Oligomerization Determination of Bovine, Mouse and Xenopus Arrestin. In preparation.

2.1 Introduction

The phototransduction cascade is terminated by the binding of visual arrestin to light-activated phosphorylated rhodopsin, followed by the termination of transducin and cGMP phosphodiesterase (PDE) activity [1]. Bovine visual arrestin has been discovered to form oligomers at physiological concentrations [2-6]. Schubert et al carried out a sedimentation equilibrium analysis of arrestin at both crystallographic and physiological concentrations [5]. Crystallography study revealed a tetrameric form of visual arrestin at high concentrations, however, this group also discovered a monomer-dimer equilibrium of visual arrestin at physiological concentrations. In addition, Shilton et al performed the small-angle X-ray scattering (SAXS) experiment to investigate the solution structure of bovine visual arrestin, demonstrating that in solution, arrestin participated a monomer-dimer equilibrium, forming dimers with a dissociation constant of 60 μM [6]. In contrast, Imamoto et al found that bovine visual arrestin went on a concentration-dependent self-association from SAXS experiment, showing that at physiological concentration, arrestin oligomerization was explained by a monomer-dimer-tetramer equilibrium [4]. Dimer concentration always remained at a low level in whole concentration range. Monomer was abundant at low concentration (<22μM) and the

amount was decreased at the concentration range between 44 μM and 176 μM. On the contrary, tetramer formation was suppressed at low concentration while it increased the proportion to the total concentration at higher concentration. This study was carried out at a physiological salt solution with the concentration of 100 mM NaCl, however, previous SAXS study performed by Shilton et al was at a high-salt concentration of 400 mM NaCl [6], which might inhibit the tetramer formation and lead to the predomination of dimer [3]. This could explain why the authors from two groups using SAXS reached contradictory conclusions. Hanson et al further confirmed the tetramerization of visual arrestin in solution by applying multiangle visible light scattering [3], which has the advantage of the independence of molecular shape due to the large light wavelength compared with the protein size [7]. Based on the data of weight-average molecular weight (MW_{av}) of bovine visual arrestin and total monomer concentrations, their group fitted the data by the monomer-dimer-tetramer (MDT) model, with dissociation constants of $K_{D,dim}$=37.2 μM and $K_{D,tet}$=7.4 μM. In addition, mouse visual arrestin was discovered to form dimers and tetramers as well [2], with higher dimerization ($K_{D,dim}$=57.5 μM) and tetramerization ($K_{D,tet}$=63.1 μM) dissociation constants compared with those of bovine ($K_{D,dim}$=37.2 μM, $K_{D,tet}$=7.4 μM) [2, 3, 8]. At the same time, the property of self-association forming dimers and tetramers was also discovered in human visual arrestin, with significantly different dissociation constants from bovine and mouse arrestins (lower $K_{D,dim}$=2.95 μM and higher $K_{D,tet}$=224 μM) [2]. Moreover, inter-subunit distance measurements were performed, indicating that rhodopsin could only bind monomeric visual arrestin, and therefore, the concentration of monomer, which could be calculated if the self-association constants were obtained, was also an important parameter [3]. Two mutations of bovine visual arrestin, Phe85Ala (F85A) and Phe197Ala (F197A), predicted to disrupt NN and CC self-association interfaces, led to a constitutive monomer, indicating the

interaction interfaces of oligomers [8]. Homologous mutations in mouse visual arrestin, Phe86Ala (F86A) and Phe198Ala (F198A) (or combined with Ala349Val (A349V)), resulted in same phenomenon with constitutive monomer as well [2], demonstrating that the interaction interfaces were conserved in both bovine and mouse arrestins. Moreover, mutations disrupting oligomerization did not affect the binding affinity of visual arrestin to light-activated phosphorylated rhodopsin and microtubules [2]. Visual arrestin was sensitive to its conformational changing by presenting significant changes in binding affinity to light-activated phosphorylated rhodopsin [9-16] and microtubules [17, 18]. However, the mutations mentioned above did not change the binding affinity to either partner, ruling out the possibility of global structural changes, indicating that the mutations only disrupted the self-association interfaces [2]. In addition, from the light scattering and electron paramagnetic resonance experiments, Hanson et al discovered that residue Phe79 (F79) was involved in inter-subunit interactions in the solution tetramer as well [3]. These residues were conserved in mammalian visual arrestin proteins [19] and it was suggested that self-association was an important property of mammalian arrestin in photoreceptors [2, 20]. However, the function of arrestin oligomerization has not been demonstrated yet.

With high expression levels in rod photoreceptors, visual arrestin, which is expressed at a ratio of ~0.8:1 to rhodopsin [21, 22], is the second most abundant signaling protein in photoreceptors [21-24]. Although many proteins are expressed at enormous by higher levels in rods than in other cells [25] and the amount of arrestin ranks second among signaling proteins in rods, visual arrestin is the only signaling protein which has an inactive storage form [2]. All the previous mechanistic research was carried on with bovine visual arrestin [14, 26], while most of the physiological studies of photoreceptor function were performed in transgenic mice [27, 28],

with the eventual goal of developing strategies for human therapy [9]. It is necessary to confirm whether bovine and mouse arrestin could self-associate and to measure the parameters of association constants of these species. Our laboratory performs a combination of live cell multiphoton & confocal imaging methods, which are novel in determining intracellular protein dynamics and carrying out quantitative analyses to understand the potential mechanisms of soluble protein transport and localization between rod subcellular compartments [29-31]. *Xenopus laevis* have been considered as one of the best experimental models for a long time, and our laboratory has also set up the experimental system with *Xenopus* rod photoreceptors. Our laboratory wants to understand whether arrestin could oligomerization *in vivo* and whether the distribution will change. So we will express wild-type arrestin and mutant arrestin which disrupts the self-association phenomenon in *Xenopus* rod. However, no paper has published before on the self-association property of *Xenopus* arrestin in solution. Therefore, whether *Xenopus* arrestin could self-associate in solution and whether mutant *Xenopus* arrestin could disrupt self-association in solution need to be determined first. In addition, using the *Xenopus* model system will allow us to examine the biological property of *Xenopus* arrestin as well.

It is also worth noting that further research needs to be carried on to determine the self-association feature of visual arrestin. Although Kim et al fitted the light scattering data to the MDT model [2], the highest concentration tested in the paper was only 20 μM, with the fitted curve only based on the data points at the concentrations lower than 20 μM and extrapolated to higher concentrations. Under these conditions the largest average molecular weight (MW_{av}) obtained was ~65 kD for mouse visual arrestin and ~82 kD for human visual arrestin, neither of which exceeded the molecular weight of the visual arrestin dimer (~90 kD) [32]. A MW_{av} of 65 kD, for example, may result from arrestin species composed of 65% monomer (~45kD), 30%

dimer (~90kD) and 5% tetramer (~180kD). However, it can also result from a mixture consisting of 55% monomer and 45% dimer. This analysis raises the possibility that tetramerization of arrestin may not occur.

In this study, the self-association phenomenon of both wild-type and mutated purified visual arrestin of several species (bovine, mouse and *Xenopus laevis*) was investigated by analytical ultracentrifugation experiment. We expressed and purified arrestins achieving concentrations in excess of 20 μM to examine if oligomers of arresting larger than dimer could be detected. Mutations in arrestin that were reported to interrupt oligomerization were also examined. While dimers were detected for arrestins of all species, tetramers were not significant at any of the concentrations examined.

2.2 Materials and Methods

2.2.1 Plasmid Construct Preparation

Several DNA constructs were prepared, including bovine wild-type arrestin, mouse wild-type arrestin, bovine mutated arrestin (F85A/F197A), mouse mutated arrestin (F86A/F198A) and *Xenopus* mutated arrestin (F78A/Y84A/F193A). Construction of these plasmids is detailed here.

2.2.1.1 Bovine and Mouse Wild-Type Arrestin Constructs Preparation

Bovine and mouse visual arrestin cDNAs in the vector of pTrc were a generous gift from Gurevich's laboratory [33]. The coding region of bovine arrestin was excised with restriction enzymes of HindIII and Not I-HF (New England Biolabs), and subcloned in the vector of pET28a which contains a hexa his-tag region and a prescision protease cleavage site. A pair of oligonucleotide primers for the insertion sequence of bovine arrestin with 1215 bp length fragment in the Polymerase Chain Reaction (PCR) were designed: Forward Primer HindIII-

bovine ArrF (5’-ctagaagcttggatgggtaaggccaataagccggcgccaaaccacg-3’) and Reverse Primer NotI-bovine ArrR (5’-ctaggcggccgctcactcatccatagccgcctcctggtctgtcttctc-3’) (Integrated DNA Technologies). The HindIII-bovine Arr-NotI repetitive insertion sequence was intended for the pair of primers to amplify 1215 bp.

The coding region of mouse arrestin (1212 bp) was excised with HindIII and XhoI (New England Biolabs) with Forwad Primer HindIII-mouse ArrF (5’-ctagaagcttggatggcagcctgcggcaagaccaataaatcccacg-3’) and Reverse Primer XhoI-mouse ArrR (5’-ctagctcgagtcactcatcctggccagcatcctcatctttcttccct-3’).

Amplification was performed in a final volume of 200 µl containing 48 Pico mole of each primer, 0.2 µmol of dNTP (New England Biolabs), 10 units of PFU polymerase (Agilent Technology), 20 µl PFU buffer (10×Concentrate, Agilent Technology) and 200 ng sample DNA. The PCR amplification reaction was carried on in thermal cycler (Eppendorf Mastercycler® thermal cyclers). The program was composed of an initial denaturation at 94 ℃ for 2 min, followed by 30 cycles of three steps containing denaturation at 94 ℃ for 45 sec, annealing of primers at 55 ℃ for 1 min and elongation at 72 ℃ for 3 min. After the 30 cycles was done, a final elongation at 72 ℃ lasted for 5 min. 30 µl amplified products of bovine and mouse arrestin were then digested overnight with HindIII & NotI-HF (10 units for each enzyme), and HindIII & XhoI (10 units for each enzyme), respectively, in a final volume of 100 µl containing 10 µl NEB Buffer 2 (10× Concentrate, BioLabs) and 1 µl BSA (100× Concentrate, BioLabs). Then the digested products were resolved by 1% agarose gel electrophoresis at 100 volts for 45 min. Gels were stained with ethidium bromide with a final concentration of 0.5 µg/ml, cut under UV tranilluminator at 320 nm wavelength, and purified with PureLink® Quick Gel Extraction Kit (Invitrogen DNA).

In the vector preparation, 20 µg blank pET28a vector was firstly digested overnight with HindIII (26 units), together with 20 µl 10× NEB Buffer 2 and 2 µl 100× BSA in a total final volume of 200 µl mixture. Then the digested product was resolved in agarose gel for 75 min, cut and purified as discussed above. In order to prepare bovine visual arrestin vector, 4 µg purified vector was then digested with NotI-HF (5.2 units) in the mixture of 10 µl 10×NEB Buffer 2 and 1 µl 100× BSA in a total final volume of 100 µl mixture. Similarly, for mouse visual arrestin, 4 µg firstly-digested vector was digested with 5.2 units of XhoI mixed in the same buffer. Afterwards, both of the two digested vectors were resolved in agarose gel, cut and purified as discussed above.

Then the digested fragments and the corresponding pET28a vectors were subjected to ligation reaction and the products were transformed to TOP10 cells by heat shock method. Various clones were screened by performing mini-preparation by QIAprep Spin Miniprep Kit (Qiagen), followed by double digestions of the corresponding enzymes mentioned above and production detection. Positive products were then analyzed by sequencing with common sequencing primers of T7 Promoter (5'-taatacgactcactataggg-3') and T7 Terminator (5'-gctagttattgctcagcgg-3') (Core facility for DNA sequencing at SUNY Upstate Medical University).

2.2.1.2 Bovine Mutated Arrestin (F85A/F197A) and Mouse Mutated Arrestin (F86A/F198A) Constructs Preparation

According to the manufactures' instruction manual (QuickChange Site-Directed Mutagenesis Kit, Agilent Technologies), a 50 µl reaction containing 50 ng template (bovine wild-type arrestin or mouse wild-type arrestin), 12 pmol of each primers, 0.05 µmol dNTP, 5 µl

PFU reaction buffer (10×concentrate), 2.5U PFU Turbo DNA polymerase (Agilent Technologies).

Each time, only one pair of primers was mixed with DNA template. The primers are summarized in Table Table **1**. The temperature cycles were as follows: incubation at 95°C for 2 min, followed by 18 cycles of 95 °C for 45 sec, 55 °C for 1 min and 68 °C for 14 min, and a final extension at 68 °C for 14 min. Next, it was digested with DpnI enzyme for 1h. The pure mutated DNA construct was then transformed into TOP10 cells and harvested by performing steps of mini-preparation. Finally, the mutated DNA construct was confirmed by sequencing.

Table 1 Primers for Site-directed Mutagenesis by Quickchange (bovine F85A/F197A, mouse F86A/F198A)

Primer Name	Primer Sequence
QC(F)F85A(bovine)	5'-ccgcagggacctctacgcttcccaggtccagg-3'
QC(R)F85A(bovine)	5'-cctggacctgggaagcgtagaggtccctgcgg-3'
QC(F)F197A(bovine)	5'-ggcctcctggcagttcgctatgtcggacaagcccc-3'
QC(R)F197A(bovine)	5'-ggggcttgtccgacatagcgaactgccaggaggcc-3'
QC(F)F86A(mouse)	5'-ccgcagggacctgtatgcttctcgggtccaggtataccc-3'
QC(R)F86A(mouse)	5'-gggtatacctggacccgagaagcatacaggtccctgcgg-3'
QC(F)F198A(mouse)	5'-gcctcctggcagttcgctatgtctgacaagcccc-3'
QC(R)F198A(mouse)	5'-ggggcttgtcagacatagcgaactgccaggaggc-3'

2.2.1.3 Xenopus Mutated Arrestin (F78A/Y84A/F193A) Construct Preparation

Xenopus visual wild-type arrestin is in the vector of pET28a. Similarly, in order to make *Xenopus* mutated arrestin (F78A/Y84A/F193A), site-directed mutagenesis by PCR quickchange was performed as mentioned above. The primers are summarized in Table Table *2*.

Table 2 Primers for Site-directed Mutagenesis by Quickchange (*Xenopus* F78A/Y84A/F193A)

Primer Name	Primer Sequence
QC(F)F78A/Y84A(*Xenopus*)	5'-attggcctaaccgcccgtaaagacctttacgccgctcggactcagatttacccacc-3'
QC(R)F78A/Y84A(*Xenopus*)	5'-ggtgggtaaatctgagtccgagcggcgtaaaggtctttacgggcggttaggccaat-3'
QC(F)F193A(*Xenopus*)	5'-gcggagacatcatggcagttcgctatgtcagacaaacctctgcacc-3'
QC(R)F193A(*Xenopus*)	5'-ggtgcagaggtttgtctgacatagcgaactgccatgatgtctccgc-3'

2.2.2 Arrestin Expression and Purification

Different species of wild-type or mutated arrestin were expressed in BL21 cells and grown in 8 l of LB culture [every liter of LB culture containing 10 g tryptone (Fisher Scientific), 5 g yeast extract (Fisher Scientific), 10 g NaCl (Fisher Scientific)and 30 mg Kanamycin (Amersco Inc.)] . It was firstly shaked at 37 ℃, 125 rpm until optical density measurement at 600 nm (O.D.A_{600}) reached 0.45-0.50, using the UV-Visible spectrophotometer (Beckman Coulter DU730). Then the temperature was lowered to 18 ℃. When O.D.A_{600} reached 0.6, 0.5 ml of Isopropyl β-D-1-thiogalactopyranoside (IPTG, Affymetrix Inc.) (1 M stock) per liter of LB culture was added and left in shaker overnight.

The next morning, cells were spun down in eight 500 ml centrifuge bottles 15 minutes at 4424 ×g at 4 ℃ (Beckman Coulter Avanti J-E). The supernatant was discarded, and more cells were added repeatedly until all cells were centrifuged. 25 ml ice-cold high-salt lysis buffer [20 mM Tris/HCl, pH 8.0 (from 1 M stock, Fisher Scientific), 0.6 M NaCl, 1 mM phenylmethylsulfonyl fluoride (PMSF, from 100 mM stock in isopropanol, Sigma-Aldrich Co.), 1 μg/ml Leupeptin (from 10 mg/ml stock), 1 μg/ml Pepstatin (from 10 mg/ml stock) and 5 mM 2-Mercaptoethanol (BME, Sigma-Aldrich Co.)] was added to each bottle. Each pellet was resuspended in high salt lysis buffer and poured into eight 50 ml conical tubes. Each tube was sonicated 4×30 seconds on Setting 5 (Fisher Scientific) and let itself sit for >1min between each sonication. Cells were then poured into eight 50 ml centrifuge round-bottom tubes and were centrifuged 30 min at 17418 ×g at 4 ℃. Supernatant was poured into new tubes and centrifugation was repeated at 17418 ×g for 30 min at 4 ℃. After the second centrifugation, supernatant was equally divided into six 50 ml conical tubes and combined with Nickel-NTA Agarose (2 ml of Ni-NTA Agarose per liter of LB culture, Qiagen) which had already been

equilibrated with column wash buffer [20 mM Tris/HCl, pH 8.0, 0.6 M NaCl and 10 % glycerol (from 50 % stock, v/v, Fisher Scientific)], and then was placed on rocker at 4 ℃ for 1 h. Later, supernatant combined with Ni-NTA agarose was poured into columns (Glass Econo-Column Chromatography Column, 1.0×30cm, Bio-Rad) and column wash buffer (50 ml per 1 l of LB culture) containing 5 mM, 10 mM, 15 mM and 20 mM imidazole (Fisher Scientic) was added into columns in sequence. 50 μg of prescission protease (purified, see below) per 1 l culture was added to ~2.5 ml prescission protease buffer (50 mM Tris/HCl, pH 7.5, 0.15 M NaCl, 1 mM Ethylenediaminetetraacetic Acid (EDTA, MP Biomedicals) and 5 mM BME) and was added equally into columns and left overnight.

The next morning, the prescission protease buffer was collected. The columns were then eluted 1 ml for five times with elution buffer without imidazole (20 mM Tris/HCl, pH 8.0, 10 mM NaCl, 5 mM BME). The first three collections and prescission protease buffer collection were combined and incubated with 1.2 ml glutathione agarose (Pierce Protein Biology) on rocker at 4 ℃ for 1 h, after leaving a little of collections for gel analysis. The fractions and glutathione agarose were then added to the column and flow-through was collected and injected into dialysis cassette (Slide-A-Lyzen Dialysis Cassette, 10,000 MWCO, Thermo Scientific) or dialysis tubing (Spectra/Por Dialysis Membrane, 12-14,000 MWCO, Spectrum Laboratories). The cassette or tubing was placed in 4 l of salt dialysis buffer (95 mM KCl (Fisher Scientific), 15 mM NaCl, 5 mM $MgCl_2$ (Fisher Scientific), 2 mM DTT (Promega Corporation), and 10 mM HEPES (Fisher Scientific), adjust to pH 7.8) with gentle stirring for 4 h and was moved to new dialysis buffer with gentle stirring overnight.

On the following morning, the solution was removed from dialysis cassette or tubing and placed in 50 ml conical tube on ice. Every 4 ml of the dialyzed sample was concentrated in

centrifugal filter (Amicon Ultra 4 ml Filters, 10,000 NMWL) in 15 min at 4108 ×g (Beckman Coulter J6-MI Centrifuge). The concentration was determined with the UV-Vis spectrophotometer by measuring its absorbance at the wavelength of 280 nm. The concentrated samples were then diluted to different desired concentrations with dialysis buffer [34].

2.2.3 PreScission Protease Expression and Purification

Prescission protease in pGEX-6P-1 vector was obtained from Dr. Ying Huang's Laboratory at SUNY Upstate Medical University. It was expressed in TOP10 cells and grown in 2 l LB culture containing 100 mg Carbenicillin (Carbenicillin DIRECT). It was firstly shaked at 37 ℃, 125 rpm until optical density measurement at 600 nm ($O.D.A_{600}$) reached values at 0.80-1.00. Then the culture was kept growing overnight at 30 ℃ after adding 1 ml IPTG (1M stock).

The next morning, the culture was centrifuged at 4424 ×g for 15 min at 4 ℃ and the pelleted cells were then resuspended in totally 20 ml lysis buffer [20 mM Tris/HCl, pH 8.0, 250 mM NaCl, 1 mM EDTA, 5 mM BME, 1 mM DTT (from 0.5 M stock), 1 µg/ml Leupeptin (from 10 mg/ml stock), 1 µg/ml Pepstatin (from 10 mg/ml stock)]. Cells were subsequently sonicated 30 seconds four times and incubated on ice between each round. The insoluble fraction was then spun down by centrifugation at 17418 ×g for 30 min at 4 ℃. The supernatant was gently poured into new tubes and spun again for 30 min. Meanwhile, 1.0 ml glutathione agarose was equilibrated in 1 ml lysis buffer and then top layer was removed. The supernatant after the second centrifugation was then combined with glutathione agarose and incubated at 4 ℃ with gentle rocking for 1 h. The mixture was poured into a column (Bio-Rad 1.0×30 cm Glass Econo-Column Chromatography Column) and washed with 300 ml wash buffer [25 mM Tris/HCl, pH 8.0, 250 mM NaCl, 1 mM EDTA, 1 mM DTT (from 0.5 M stock), and 0.2 mM PMSF (from 100 mM stock in isopropanol)]. The GST-prescission protease fusion protein was then eluted

from the beads with 8 ml elution buffer [25 mM Tris/HCl, pH 8.0, 250 mM NaCl, 1 mM EDTA, 1 mM DTT (from 0.5 M stock), 20 mM Glutathione Reduced (from 0.2 M stock, Sigma-Aldrich Co.), 0.2 mM PMSF (from 100 mM stock in isopropanol)], which was added 1ml each time and incubated on the column for 15 min. Fractions were collected each time and combined to be dialyzed in 4 l dialysis buffer [25 mM Tris/HCl, pH 8.0, 250 mM NaCl, 1 mM EDTA, 1 mM DTT (from 0.5 M stock), and 0.2 mM PMSF ((from 100 mM stock in isopropanol)] overnight at 4 ℃.

On the third morning, the solution was removed from dialysis cassette or tubing and then the solution was placed in 50 ml conical tube on ice. The concentration of the solution was determined with the UV-Vis spectrophotometer by measuring its absorbance at the wavelength of 280 nm. The prescission protease was stored in glycerol at the final concentration of 20 % (v/v) and concentrated, and then was frozen in 0.1 ml aliquots in the -20 ℃ freezer.

To test the cleavage activity of purified prescission protease, various amounts were incubated with equal amounts of resin (EGFP bound to Ni-NTA Agarose), which was followed by taking an equal amount of supernatant to run on a Coomassie blue gel.

To test the binding affinity of prescission protease with glutathione agarose, 50 µl prescission protease was mixed with 50 µl glutathione agarose and 5 µl supernatant was taken immediately after the comination. After 1 h, the mixture was centrifuged at 5000 ×g for 10 min in 4 ℃ and 5 µl supernatant was taken as well. Both supernatants were then loaded on the Coomassie blue gel.

2.2.4 SDS-PAGE (Coomassie blue staining) and Western Blot Analysis

Concentrated proteins were separated on SDS-PAGE [15 % separating gel: 3.56 ml dH2O, 3.75 ml 40 % Acrylamide (Bio-Rad Laboratories), 2.50 ml 1.5 M Tris/HCl, pH 8.8, 100

µl 10 % sodium dodecyl sulfate (SDS, Bio-Rad Laboratories), 100 µl 10 % Ammonium persulfate (APS, Bio-Rad Laboratories) and 10 µl N, N, N', N'-tetramethylethylenediamine (TEMED, Bio-Rad Laboratories); 6 % stacking gel: 5.80 ml dH_2O, 1.50 ml 40% Acrylamide, 2.50 ml 0.5 M Tris/HCl, pH 6.8, 100 µl 10% SDS, 100 µl 10% APS and 10 µl TEMED] using the buffer system of Laemmli [35]. Gels were run at a constant voltage of 200 V in 500 ml Tris-Glycine running buffer [containing 7.2 g Glycine (Fisher Scientific), 1.515 g Tris Base and 0.5 g SDS].

For protein gel, it was stained in Coomassie blue gel stain buffer (0.25 % coomassie blue R Sigma-Aldrich Co.), 50 % MeOH (Ultra-Pure, LLC) and 10 % acedic acid (Fisher Scientific)) overnight. It was then destained by gel destain buffer (10 % acetic acid and 50 % MeOH) and scanned [36].

For western blot analysis, after electrophoresis was complete, the gel was transferred to an immobilon transfer membrane (Millipore, #IPVH00010, pore size 0.45 µm) by running at 27 V for 2 h in 1 l transfer buffer (14.4 g Glycine and 3.03 g Tris Base). Then the membrane was blocked in 20 ml blocking buffer [1× PBS (from 10× stock), 0.05% Tween-20 (from 10 % stock, Fisher Scientific) and 5 % dry milk (Nestle)] by gently rocking overnight in 4 ℃. Membrane was washed with wash buffer [1× PBS and 0.1 % Tween-20 (from 10 % stock)] and then incubated in blocking buffer containing 0.03 % rabbit-anti-arrestin antibody as the primary antibody for 1 h at room temperature. The membrane was washed again and incubated with secondary antibody in blocking buffer containing 0.01 % mouse-anti-rabbit-HRP antibody for another 1 h at room temperature. The membrane was then incubated with enhanced chemiluminescence (ECL) western blotting substrate (Pierce Protein Biology Product, Thermo Scientific) and scanned via Biorad ChemiDoc XRS^+ System.

2.2.5 Analytical Ultracentrifugation

The sedimentation velocity analytical ultracentrifugation (AUC) experiments were performed by Stephen Shinsky and Anamika Patel from Dr. Michael Cosgrove's laboratory at SUNY Upstate Medical University. The analytical ultracentrifuge is till now one of the most accurate methods to measure the molecular weight of a protein and to determine its hydrodynamic and thermodynamic characteristics in solution [37]. It is able to determine the sedimentation coefficient, the diffusion coefficient and molecular mass of molecules with different sizes [38]. Sedimentation velocity, one of the AUC methods, determines the velocity of molecule movement in response to a huge centrifugal force inside the centrifuge, which provides data related to the molecular mass and shape of molecules [39]. Arrestin samples were diluted into different desired concentrations in 120 mM salt dialysis buffer (95 mM KCl, 15 mM NaCl, 5mM $MgCl_2$, 2 mM DTT, and 10 mM HEPES, adjust to pH 7.8). Experiments were performed at 10 ℃ with Beckman Coulter ProteomLab XL-A analytical ultracentrifugation equipped with absorbance detection at 230 nm and a four-hole An-60 Ti rotor at 60,000 rpm (262,000 ×g). The arrestin samples were scanned with the time interval between scans being zero for 300 scans and analyzed by the continuous distribution method c(s) in the program SEDFIT [40].

By using the Sedphat software, the protein self-association analysis could be obtained from the isotherm of weight-average sedimentation coefficients S_w as a function of arrestin concentrations, allowing the determination of thermodynamic information of arrestin self-association in solution. Various self-association models for global analysis were chosen in to find the best model fitting the data [41].

2.2.6 Generation of Transgenic Xenopus Using Restriction Enzyme-Mediated Integration (REMI)

REMI reaction was performed by the mixture of sperm nuclei, egg extract, linearized plasmid and restriction enzyme [42-44]. After the REMI reaction, microinjection of sperm nuclei into eggs were performed [45]. Then fertilized eggs were selected and well-developing embryos were sought out at different stages until the 7th day when they were able to be sorted under the dissecting microscope with UV light [44].

2.3 Results

2.3.1 Purification of PreScission Protease

SDS-PAGE with Coomassie blue staining was used to confirm the purity of prescission protease after purification (Fig. 1A). Only one band appeared on the gel, which was located between 37 kD and 50 kD standards, indicating that there was no contamination in the precision protease purification. Then 0 µl, 5 µl, 10 µl and 25 µl of purified prescision protease were incubated overnight with 270 µl resin (EGFP bound to Ni-NTA Agarose), respectively, and after centrifugation, 5 µl supernatant was loaded on the gel. The cleavage activity of purified prescission protease was shown from Coomassie blue gel (Fig. 1B). As expected, 0 µl purified prescission protease did not cleave any EGFP from Ni-NTA Agarose, and 5 µl purified prescission protease did not cleave much EGFP from Ni-NTA agarose either, while 10 µl purified prescission protease cleaved some EGFP and 25 µl purified prescission protease cleaved more EGFP, with one band at ~25 kD indicating EGFP and the other band between 37 kD and 50 kD showing redundant purified prescission protease, suggesting that the prescission protease exceeded the need for EGFP cleavage and confirming the cleavage activity of prescission protease.

To test the binding affinity of prescission protease with glutathione agarose, 5 µl supernatant was taken promptly after the mixture of 50 µl glutathione agarose and 50 µl prescission protease. Centrifugation was performed after 1 h combination, and 5 µl supernatant was taken as well. Fig. 1C confirms the binding affinity of prescission protease with glutathione agarose. A faint band appeared (Fig. 1C, lane c), but when compared with the band in lane b (Fig. 1C), the protein gel still indicated that most of the prescission protease was able to bind glutathione agarose within 1 h.

It was worth noting that prescission protease should be stored in 20 % glycerol (v/v) to prevent it from aggregation and to maintain its activity [46]. The several upper bands in lane b (Fig. 1D) demonstrated that prescission protease was easily aggregated if it was not stored in glycerol.

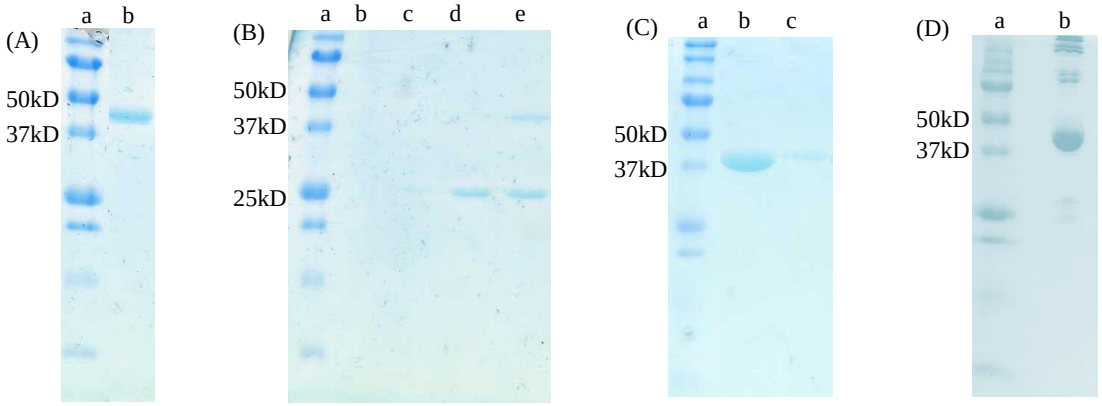

Figure 1. Determination of prescission protease purity and activity. (A) Purified prescission protease was subjected to SDS-PAGE and visualized by Comassie blue staining as described in Methods. (a) Precision Plus Protein all blue standard. (b) Purified prescission protease was shown as only one band. (B) Cleavage activity of purified prescission protease was tested. (a) Precision Plus Protein all blue standard. (b)-(e) 0 µl, 5 µl, 10 µl and 25 µl of purified precision protease were incubated overnight with 270 µl resin, respectively, and after centrifugation, 5 µl supernatant was loaded on the gel. (C) Binding affinity of purified prescission protease with glutathione agarose was tested. (a) Precision Plus Protein all blue standard. (b) Supernatant taken immediately after mixing prescission protease and glutathione agarose. (c) Supernatant taken after 1 h mixing of prescission protease and glutathione agarose. (D) The aggregation of prescission protease without storing in glycerol was tested. (a) Precision Plus Protein all blue standard. (b) Multiple bands shown in prescission protease without storing in glycerol.

2.3.2 Different Species of Arrestin Purification

Experiments of Coomassie protein gel and western blot were performed to test the arrestin purity, and only purified arrestin could be used to perform the analytical centrifugation experiment. Only one band appeared on the Coomassie blue protein gel of each arrestin species (Fig. 2A-D, lane a), indicating the protein was purified and qualified for the analytical centrifugation experiment. Western blot was performed as well, and arrestin was detected by arrestin antibody (Fig. 3A-D, lane a), confirming that the purified protein was arrestin.

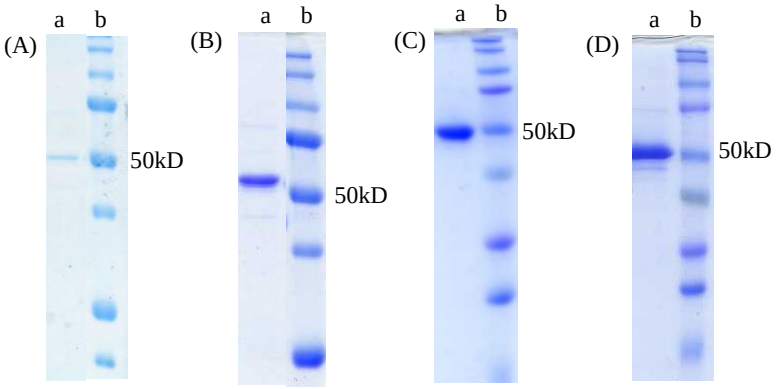

Figure 2. Determination of arrestin purity with Coomassie blue protein gel. (A)-(D) are bovine wild-type arrestin, mouse wild-type arrestin, *Xenopus* wild-type arrestin, and *Xenopus* mutated arrestin (F78A/Y84A/F193A), respectively. (a) Purified arrestin was shown as only one band. (b) Precision Plus Protein all blue standard in A-B and Precision Plus Protein Kaleidoscope Standards in (C) and (D).

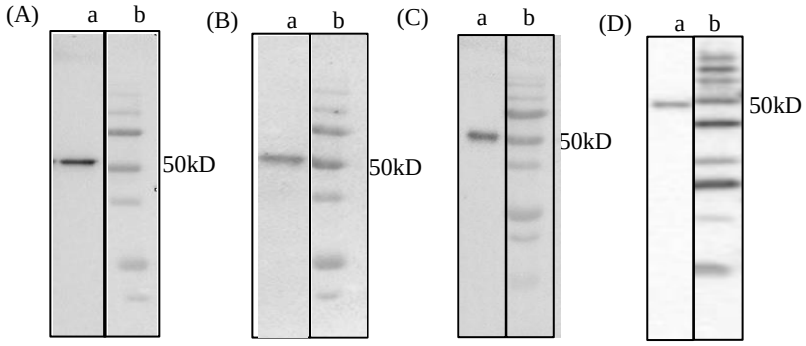

Figure 3. Western Blot Analysis for purified arrestin. (A)-(D) are bovine wild-type arrestin, mouse wild-type arrestin, *Xenopus* wild-type arrestin, and *Xenopus* mutated arrestin (F78A/Y84A/F193A), respectively. (a) Purified arrestin was detected as the only signal. (b) Precision Plus All Blue Standard was used in (A)-(C) and Precision Plus Protein WesternC Standards was used in (D).

2.3.3 Determination of Arrestin Self-association

The self-association property of visual arrestin of different species at micromolar concenrations was investigated using sedimentation velocity experiments. Data sets collected at multiple concentrations were carried out using Sedfit program and the weight-average sedimentation coefficients were obtained at the corresponding concentrations. For wild-type arrestin of all three species (bovine, mouse and *Xenopus*), the results of sedimentation coefficient distributions from the analysis of the sedimentation profiles (crossing in Fig. 4A, C and E) suggested that they possessed the self-association characteristic of forming at least dimers, indicating that the performance of analytical ultracentrifugation experiment was feasible in determining the oligomerization phenomenon of arrestin. Isotherms of weight-average sedimentation coefficient as a function of concentrations were fitted to both Monomer-Dimer Self-Association (MD, $2M \underset{K_{D,dim}}{\overset{K_{dim}}{\rightleftharpoons}} D$) and Monomer-Dimer-Tetramer Self-Association (MDT, $2D \underset{K_{D,tet}}{\overset{K_{tet}}{\rightleftharpoons}} T$) models, however, no significant differences of the two fittings were observed. From Table 3, the data of bovine wild-type arrestin was fitted to MD model with $K_{D,dim=}$736.4 μM, however, was fitted to MDT model with a $K_{D,dim}$=686.3 μM and $K_{D,tet}=4.8\times10^{10}$ μM. The data of mouse wild-type arrestin had a $K_{D,dim}$=1127.0 μM when fitted to MD model while had a $K_{D,dim}$=1110.5 μM and a $K_{D,tet}=1.3\times10^{10}$ μM when fitted to MDT model. For *Xenopus* wild-type arrestin, the $K_{D,dim}$ was 80.8 μM of the MD model while the $K_{D,dim}$=80.6 μM and $K_{D,tet}=1.9\times10^{7}$ μM of the MDT model. The data also suggested that the arrestin formed unstable oligomers in fast self-association and dissociation system, which could be indicated from the sedimentation coefficient peak positions dependent on protein concentrations. Interestingly, the mutant *Xenopus* arrestin (3A), which was proposed to be constitutive monomer as well, still self-associated with similar phenomenon of wild-type *Xenopus* arrestin, although with a lower

affinity. *Xenopus* (F78A/Y84A/F193A) arrestin yielded a $K_{D,dim}$=200.7 μM when fitted to MD model, and a $K_{D,dim}$=199.8 μM and a $K_{D,tet}$=2.8×10^{8} μM when fitted to MDT model (Fig. 4G). Fig. 4B, D, F and H showed the percentage of the visual arrestin of the corresponding species in monomer and dimer forms as a function of total arrestin concentration computed for the MD model. It was observed that the root-mean-square deviations of the MD fitting and the corresponding MDT fitting were the same in bovine wild-type arrestin, as well as the mouse wild-type arrestin (Table 3, the first two lines). Similarly, both *Xenopus* wild-type and mutated arrestins fitted to both two models as well (Table 3, the third and fourth line). In the MDT model, all arrestin types were found with a low $K_{D,dim}$ and a remarkable high $K_{D,tet}$. Because the data was fitted to MD and MDT models equally well, there was no reason for us to suggest the existence of tetramer. However, the current data was still able to prove that bovine, mouse and *Xenopus* wild-type arrestin could robustly self-associate at physiological concentrations, indicating that this property might have biological importance. In addition, by comparing the dissociation constant of the mutated arrestin with that of wild-type arrestin, the dimerization in mutated arrestin was inhibited at some extent but not completely absent.

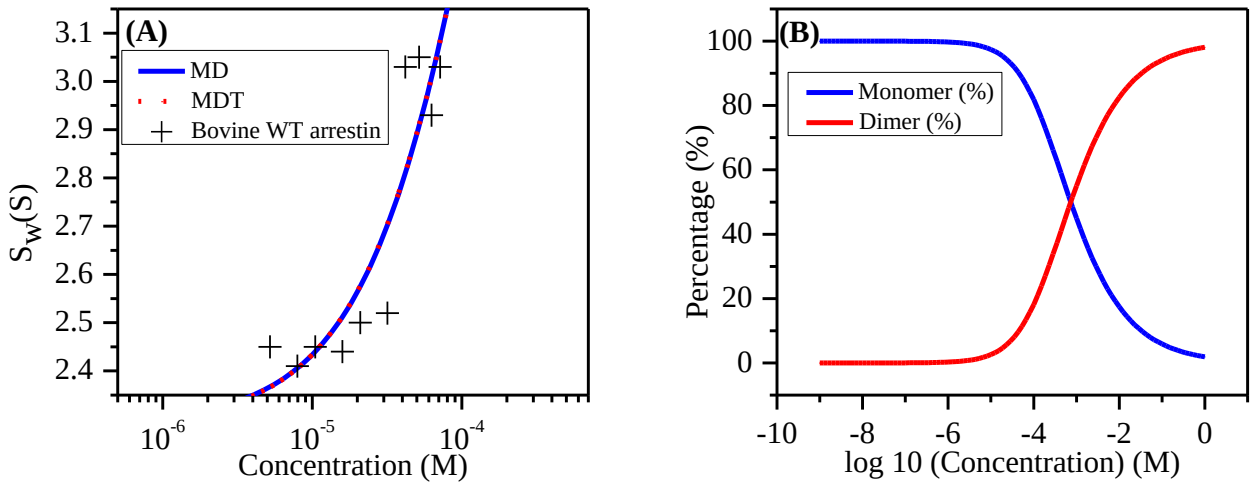

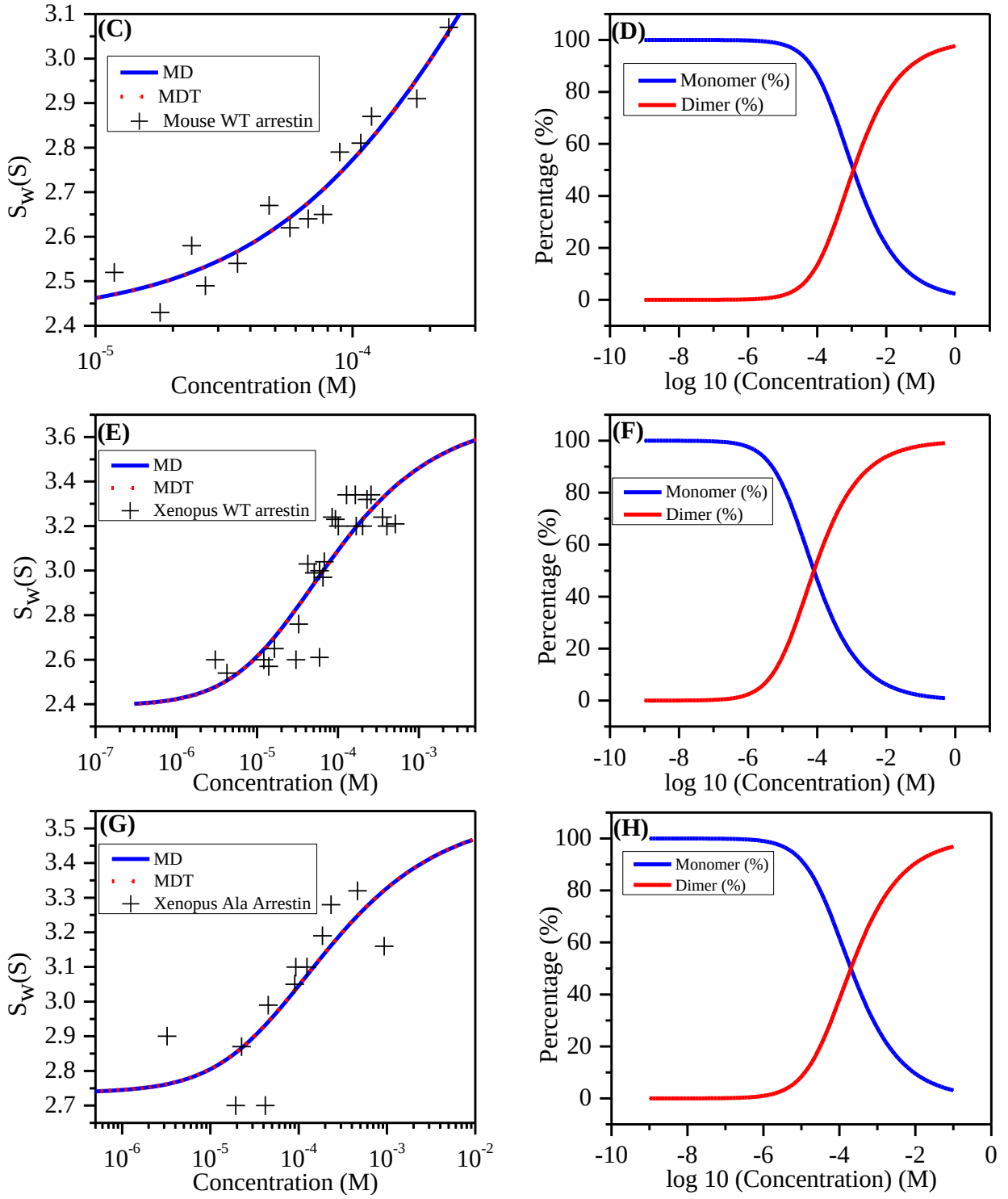

Figure 4. Wild-type bovine, mouse, Xenopus and Xenopus mutated (F78A/Y84A/F193A) arrestins fitted to the MD and MDT models. (A), (C), (E) and (G) are the isotherms of the four arrestins of weight-average sedimentation coefficient as a function of concentration (black crossings). (B), (D), (F) and (H) present the percentage of the four arrestin molecules in monomer (M) and dimer (D) forms as a function of total arrestin concentration computed for the MD model and the data in panel (A), (C), (E) and G, respectively.

Table 3 Equilibrium constants characterizing self-association of bovine wild-type, mouse wild-type, *Xenopus* wild-type and *Xenopus* mutated (F78A/Y84A/193A) arrestins.

protein	MD model		MDT model		
	$K_{D,dim}$ (μM)	rmsd	$K_{D,dim}$ (μM)	$K_{D,tet}$ (μM)	rmsd
Bovine WT Arrestin	736.4	0.1136	686.3	4.8×10^{10}	0.1136
Mouse WT Arrestin	1127	0.0451	1110.5	1.3×10^{10}	0.0451
Xenopus WT Arrestin	80.8	0.1332	80.6	1.9×10^{7}	0.1332
Xenopus Arrestin (F78A/Y84A/F193A)	200.7	0.1126	199.8	2.8×10^{8}	0.1126

Xenopus laevis rod outer segment has the mean length of 60 μm [25, 47, 48] with the diameter of 6 μm [25, 48]. The length and the diameter of the inner segment are both considered to be 6 μm in the following calculation based on the data from our laboratory. Approximately regarded as a cylindrical shape as a whole with negligible volume of connecting cilium, the envelope volume of the entire rod was 1.87×10^{-12} l calculated according to Equation (1). Rod photoreceptor was shown to possess 3×10^{9} rhodopsin molecules [25], and the expression level of visual arrestin and rhodopsin was similar [21, 22], therefore, for simplification, the amount of arrestin molecules in rod photoreceptor could also be considered as 3×10^{9}. Based on the envelope volume of entire rod photoreceptor, the effective concentration of arrestin in the entire rod in the dark-adapted state, which is proposed to be the same in rod inner segment and outer segment, is 2.67 mM calculated based on Equation (2).

$$V_{total}=\pi\times r^{2}\times(l_{OS}+l_{IS}) \quad (1)$$

$$C=\frac{N/N_{A}}{V_{total}} \quad (2)$$

Where V_{total} is the envelope volume of the entire rod photoreceptor; r is the radius of outer and inner segment; l_{OS} and l_{IS} denotes the lengths of the outer segment and the inner segment, respectively; C is the effective concentration of arrestin in the entire rod based on the

envelope volume; and N is the total amount of arrestin molecules in rod photoreceptor and N_A is the Avogadro Constant.

With similar arrestin expression level in all the arrestin species in the dark-adapted state [23, 49], *Xenopus* arrestin expression level was used to estimate the monomer and dimer percentages in the entire rod with the arrestin concentration of ~2.7 mM based on the envelope volume of rod. The disparate equilibrium constants of the three wild-type arrestin species yielded predicted levels of monomer and dimer at a total arrestin concentration of 2.7 mM, demonstrating high dimer percentage (69.0 %, 63.6 % and 88.5 %, respectively) and lower monomer percentage (31.0 %, 36.4 % and 11.5 %, respectively) (Table 4). In addition, the predicted mutated arrestin expression level also showed higher dimer percentage in the outer segment (82.5 %) and lower monomer percentage (17.5 %) at the concentration of 2.7 mM (Table 4).

Table 4 Predicted concentrations and percentages of the monomer and dimer of bovine wild-type, mouse wild-type, *Xenopus* wild-type and mutant *Xenopus* (3A) arrestins in entire rod photoreceptor (2.7 mM) in the dark-adapted state.

protein	Entire Rod (2.7 mM)	
	[Monomer](μM) (% of total)	[Dimer](μM) (% of total)
Bovine WT Arrestin	836.9 (31.0 %)	931.5 (69.0%)
Mouse WT Arrestin	983.5 (36.4%)	858.2 (63.6%)
Xenopus WT Arrestin	309.9 (11.5%)	1195.0 (88.5%)
Mutant *Xenopus* (3A)	472.8 (17.5%)	1113.6 (82.5%)

Outer segment contained thousands of disks [50] which occupied half volume of the outer segment [51]. As discussed above, the effective concentration of arrestin (2.7 mM) was based on the envelope volume of the entire rod. However, when thinking about the disk excluded volume, the effective concentration of arrestin was ~2-fold (for simplification) of 2.7 mM, given the value of ~5.4 mM in the entire rod photoreceptor. Furthermore, when considering steric

volume exclusion, the concentration was even higher, reaching ~4-fold of 2.7 mM, given the effective concentration of ~10 mM with the dimer percentage at least ~80 % in all four types of arrestins (Table 5).

Table 5 Predicted concentrations and percentages of the monomer and dimer of bovine wild-type, mouse wild-type, *Xenopus* wild-type and mutant *Xenopus* (3A) arrestins in entire rod photoreceptor (10 mM, considering steric volume exclusion) in the dark-adapted state.

protein	Entire Rod (10 mM, considering steric volume exclusion)	
	[Monomer](μM) (% of total)	[Dimer](μM) (% of total)
Bovine WT Arrestin	1743.4 (17.4%)	4128.3 (82.6%)
Mouse WT Arrestin	2101.8 (21.0%)	3949.1 (79.0%)
Xenopus WT Arrestin	615.7 (6.2%)	4692.2 (93.8%)
Mutant *Xenopus* (3A)	952.9 (9.5%)	4523.5 (90.5%)

2.4 Discussion

Arrestin has been shown for more than thirty years that it binds to light-activated phosphorylated rhodopsin, where it terminates rhodopsin signaling [52, 53]. Several years earlier than this observation, arrestin self-association was firstly discovered by sedimentation velocity experiment [54]. The phenomenon of self-association was confirmed both in crystal structures [55, 56] and in solution [3-5], however, the tetramer structure in the solution was shown to be significantly different from that found in crystal. From previous study with electron paramagnetic resonance experiment, residues I72, F79, L173 and T233 were at or near the tetramer interface in solution, however, they did not make any contacts in the crystal structure [3]. In addition, V224 was shown at the interface of solution tetramer, but was not at crystal contacts either. Only arrestin in monomeric form was able to bind light-activated phosphorylated rhodopsin [3], demonstrating that the oligomers might function as the storage form of arrestin. Previous research using multiangle light scattering suggested that mouse visual arrestin self-

associated, existing in a monomer-dimer-tetramer equilibrium [57]. Bovine visual arrestin formed oligomers as well, however, it was still difficult to determine whether it could form tetramer or not [3-5]. Moreover, it is also not clear whether self-association is a common feature of amphibian animals including *Xenopus laevis*, or is only a peculiar phenomenon in mammalian animals.

In this chapter, the self-association phenomena of visual arrestin from bovine, mouse and *Xenopus laevis* were compared by performing analytical ultracentrifugation experiments. Bovine was chosen as one of the three experimental subjects because previous studies always used bovine for biochemical properties of visual arrestin. Mouse visual arrestin was also studied because most functional studies *in vivo* were performed on mice. Analytical ultracentrifugation is a powerful method for the quantitative analysis of molecular interactions in solution, among which, sedimentation velocity experiments are able to determine the concentration-dependent self-association reactions [58]. By comparing the results with previous studies on bovine and mouse arrestins [2-5], the practicability of performing sedimentation velocity experiments were confirmed to demonstrate the self-association property of bovine and mouse visual arrestins. *Xenopus* arrestin was chosen as well because it was one of the best animal models in live cell multiphoton & confocal imaging methods. In each species, visual arrestin was found to oligomerize at physiological concentrations, indicating the biological importance of self-association. Dimerization was observed in all three species, however, tetramers were not unequivocally observed. In addition, the dissociation constants of each species were significantly different. When fitted to the MD model, the value of measured dissociation constants between bovine and *Xenopus* arrestins showed a ~9-fold difference, and the $K_{D,dim}$ between mouse and *Xenopus* proteins differed by ~14-fold. Homologous residues determined in bovine arrestin that

block self-association were discovered not to be conserved in *Xenopus* proteins. Thus the solution structure of *Xenopus* arrestin oligomers would need further investigation.

Previous multiangle light scattering experiment demonstrated that bovine and mouse arrestins were fitted to MDT model with $K_{D,dim}$=37.2 μM and $K_{D,tet}$=7.4 μM for bovine arrestin, and $K_{D,dim}$=57.5 μM and $K_{D,tet}$=63.1 μM for mouse arrestin [2]. Our result was different from the previous study, showing that bovine and mouse arrestins were fitted to MD and MDT models equally well. Hence, our data might not be able to suggest the existence of tetramer. By fitting to the MD model, the dissociation constants of bovine arrestin was 736.4 μM and mouse arrestin possessed the dissociation constant of 1127.0 μM. The dissociation constants of these two species obtained in my study were both 20-fold of the dimer dissociation constants in published result. Several possibilities might cause this significant differences of the dissociation constants between my result and previous study. Firstly, the previous published data was based on the concentration lower than 20 μM and then extrapolated to higher concentrations. However, in my experiment, the highest concentrations obtained was ~100 μM for bovine arrestin and ~200 μM for mouse arrestin. Secondly, contamination in the tested sample could affect the result of scattering experiment, however, analytical ultracentrifugation could reduce this effect by only choosing the peak of arrestin. Another possibility might lead to the inaccurate result in my experiment. The measurement of arrestin concentration in my study might not be accurate due to the existence of the unfolded arrestin accompanied with the active arrestin, leading to the inaccurate fitting to the models and the incorrect dissociation constants obtained.

Rod photoreceptors are responsible for vision at low light levels [60]. Previous studies of arrestin distribution in dark-adapted rods were performed on mouse, indicating that arrestin was predominately localized in the inner segment in dark-adapted state [21, 22]. The phenomenon of

arrestin translocation from rod inner segment to outer segment in response to light and back to the inner segment in the dark has been discovered for more than twenty years [36, 61, 62]. However, the mechanism of arrestin translocation between rod subcellular compartments has not been determined yet [1]. Some people suggested that active transport was involved by showing that arrestin translocation required ATP and was an energy-dependent process [63-66] while other studies showed the contrary result, indicating that it was an energy-independent process [67]. However, if active transport was indeed the case, the translocation of arrestin, which moved 1000-fold faster than the motor-driven delivery of rhodopsin into rod outer segments [22], would saturate the capacity of molecular motors rapidly, unless arrestin moved in large aggregates or vesicles; however, such aggregates had not been found yet [1], indicating active transport could not be the mechanism of arrestin translocation. Studies have shown that in the dark-adapted state, the distribution of the arrestin-EGFP fusion protein was different from that of the soluble EGFP [68], and arrestin was able to bind to microtubules *in vitro* [18, 67, 69]. Hence, people proposed that the mechanism of the light-driven translocation of arrestin was the "competitive, two binding sinks" model, in which the mechanism could be explained as a simple competition between low affinity microtubule binding sites in the inner segment and high affinity rhodopsin binding sites in the outer segments [1]. However, with the concentration of ~50 μM in neural cells [70], α-tubulin is significant lower than he millimolar levels of arrestin [22]. In addition, the other two binding partners in the inner segment, enolase 1 and N-ethylmaleimide-sensitive factor (NSF), were ruled out as well because of the low concentration of enolase 1 at ~5 μM in rods [71] and NSF being not co-localized with arrestin in rods [72]. Therefore, the mechanism by which arrestin translocated from rod outer segment to inner segment could not be the binding affinity to microtubule, enolase 1 or NSF. Hence, even though the binding of arrestin to light-activated

phosphorylated rhodopsin was the most possible mechanism of light-driven movement of arrestin to outer segment, the mechanism of arrestin movement back to inner segment could not be the low affinity to the binding partners in the inner segment. Another hypothesis was proposed, demonstrating that a diffusion barrier in the ciliary transition zone which prevented proteins from moving to the outer segment without active transport machinery [66, 73], however, this hypothesis was later defeated. The mobility of photoactivatable green fluorescent protein (PAGFP), which was a soluble protein, was determined in the connecting cilium (CC), rod inner segment (IS) and outer segment (OS) of *Xenopus* rod by using confocal and multiphoton microscopy [31]. The diffusion coefficients of CC (D_{cc}=2.5 $\mu m^2/s$) was shown only half of D_{IS} (5.2 $\mu m^2/s$), and because PAGFP diffused more rapidly in IS than any other compartments, CC was not possible to contain a distinct diffusion barrier to soluble protein movement, including arrestin [31]. Moreover, recent study in our laboratory found that the fluxes of monomer and 3×PAGFP through the cilium transition zone were not significantly different with sizes, further confirming that no diffusion barrier was existed in the ciliary transition zone [29].

Our laboratory also studied the distribution patterns of soluble GFP monomers, dimers and trimmers which were expressed in *Xenopus* rod photoreceptors and were able to move through the connecting cilium and translocate between rod subcellular compartments [29]. The result showed that in the steady-state and compared with calcein which was a small soluble protein, GFP monomers existed in the outer segment at 1.8-fold lower abundance relative to that in the inner segment; however, GFP dimers and trimmers were present at 2.9- and 6.8-fold, respectively, indicating that distribution of GFP to the rod outer segment depended on its molecular size. Our laboratory then introduced “steric volume exclusion” idea, which posited the protein size-dependent compartmental partitioning as the mechanism for the control of soluble

protein access to the rod outer segment. Arrestin has been shown to self-associate at physiology concentrations for decades [2] and the result presented in this chapter bolstered this property. In addition, the molecular sizes of 2×GFP (27 kDa for GFP monomer and 54 kDa for GFP dimer [74]) and arrestin monomer (48 kDa [75]) were remarkably similar. Based on the result in this chapter and previous studies in our laboratory, it was suggested that the mechanism for the light-driven translocation of arrestin involved free diffusion through the connecting cilium with local binding partner of light-activated phosphorylated rhodopsin in the outer segment, and translocation to the inner segment was via steric volume exclusion, which provided a superior solution to the long-standing problem.

In summary, in this chapter, the property of visual arrestin self-association is shown to be conserved both in mammalian species (bovine and mouse) and an amphibian species (*Xenopus* laevis), suggesting that this property has biological importance. Although the tetramerization equilibrium constants are extremely high and the dimerization equilibrium constants are different in each species, it could still be confirmed that arrestin oligomerizes at physiological concentrations. Moreover, the *Xenopus* mutant protein, which was proposed to disrupt the self-association interfaces and become essentially monomerical, is found to self-associate as well and has the dissociation constants shifted to a 2.5-fold higher value, indicating that the self-association interfaces are not conserved in amphibian animals including *Xenopus laevis*. Also, the dimer percentage is at least twice of the monomer percentage of all four types of arrestin at physiological concentrations. The importance of visual arrestin self-association demonstrates that together with the steric volume exclusion mechanism, it is probably sufficient to explain the distribution pattern in dark-adapted rods.

2.5 Conclusions

Visual arrestin self-association was shown to be conserved in bovine, mouse and *Xenopus laevis*, indicating the biological significance of this phenomenon. Results showed that, even though the equilibrium constants were different in the three species, the data fitted equally well to both MD and MDT models and as a result, it might not be suggested the tetramer formation. Despite the variations in the thermodynamics of association of different species, the percentage of the dimer was higher than that of monomer at the concentration of 2.7 mM. Mutations in *Xenopus* arrestin (F78A/Y84A/F193A) did not form constitutive monomer as expected, suggesting that these regions were not conserved in *Xenopus laevis* arrestin.

Acknowledgement

This work was supported by NIH funding, Research Prevent Blindness and Lion Club of Central New York.

Reference

1. Calvert, P.D., et al., *Light-driven translocation of signaling proteins in vertebrate photoreceptors.* Trends in Cell Biology, 2006. **16**(11): p. 560-568.
2. Kim, M., et al., *Robust self-association is a common feature of mammalian visual arrestin-1.* Biochemistry, 2011. **50**(12): p. 2235-42.
3. Hanson, S.M., et al., *Structure and function of the visual arrestin oligomer.* EMBO J, 2007. **26**(6): p. 1726-36.
4. Imamoto, Y., et al., *Concentration-Dependent Tetramerization of Bovine Visual Arrestin.* Biophysical Journal, 2003. **85**(2): p. 1186-1195.
5. Schubert, C., et al., *Visual arrestin activity may be regulated by self-association.* J Biol Chem, 1999. **274**(30): p. 21186-90.
6. Shilton, B.H., et al., *The solution structure and activation of visual arrestin studied by small-angle X-ray scattering.* Eur J Biochem, 2002. **269**(15): p. 3801-9.
7. Mogridge, J., *Using light scattering to determine the stoichiometry of protein complexes.* Methods Mol Biol, 2004. **261**: p. 113-8.
8. Hanson, S.M., et al., *A model for the solution structure of the rod arrestin tetramer.* Structure, 2008. **16**(6): p. 924-34.
9. Song, X., et al., *Enhanced arrestin facilitates recovery and protects rods lacking rhodopsin phosphorylation.* Curr Biol, 2009. **19**(8): p. 700-5.
10. Gurevich, V.V., *The selectivity of visual arrestin for light-activated phosphorhodopsin is controlled by multiple nonredundant mechanisms.* J Biol Chem, 1998. **273**(25): p. 15501-6.
11. Hanson, S.M. and V.V. Gurevich, *The differential engagement of arrestin surface charges by the various functional forms of the receptor.* J Biol Chem, 2006. **281**(6): p. 3458-62.
12. Gurevich, V.V. and J.L. Benovic, *Visual arrestin binding to rhodopsin. Diverse functional roles of positively charged residues within the phosphorylation-recognition region of arrestin.* J Biol Chem, 1995. **270**(11): p. 6010-6.
13. Gurevich, V.V. and J.L. Benovic, *Mechanism of phosphorylation-recognition by visual arrestin and the transition of arrestin into a high affinity binding state.* Mol Pharmacol, 1997. **51**(1): p. 161-9.
14. Gray-Keller, M.P., et al., *Arrestin with a single amino acid substitution quenches light-activated rhodopsin in a phosphorylation-independent fashion.* Biochemistry, 1997. **36**(23): p. 7058-63.
15. Vishnivetskiy, S.A., et al., *How does arrestin respond to the phosphorylated state of rhodopsin?* J Biol Chem, 1999. **274**(17): p. 11451-4.
16. Vishnivetskiy, S.A., et al., *An additional phosphate-binding element in arrestin molecule. Implications for the mechanism of arrestin activation.* J Biol Chem, 2000. **275**(52): p. 41049-57.
17. Hanson, S.M., et al., *Arrestin mobilizes signaling proteins to the cytoskeleton and redirects their activity.* J Mol Biol, 2007. **368**(2): p. 375-87.
18. Hanson, S.M., et al., *Visual arrestin binding to microtubules involves a distinct conformational change.* J Biol Chem, 2006. **281**(14): p. 9765-72.
19. Gurevich, E.V. and V.V. Gurevich, *Arrestins: ubiquitous regulators of cellular signaling pathways.* Genome Biol, 2006. **7**(9): p. 236.
20. Gurevich, V.V., et al., *The functional cycle of visual arrestins in photoreceptor cells.* Prog Retin Eye Res, 2011. **30**(6): p. 405-30.

21. Hanson, S.M., et al., *Each rhodopsin molecule binds its own arrestin.* Proc Natl Acad Sci U S A, 2007. **104**(9): p. 3125-8.
22. Strissel, K.J., et al., *Arrestin translocation is induced at a critical threshold of visual signaling and is superstoichiometric to bleached rhodopsin.* J Neurosci, 2006. **26**(4): p. 1146-53.
23. Song, X., et al., *Arrestin-1 expression level in rods: balancing functional performance and photoreceptor health.* Neuroscience, 2011. **174**(0): p. 37-49.
24. Chen, J., *The physiological roles of arrestin-1 in rod photoreceptor cells.* Handb Exp Pharmacol, 2014. **219**: p. 85-99.
25. Pugh Jr, E.N. and T.D. Lamb, *Phototransduction in vertebrate rods and cones: Molecular mechanisms of amplification, recovery and light adaptation.* Handbook of Biological Physics. Molecular Mechanisms in Visual Transduction, 2000. **3**: p. 183-255.
26. Wilden, U., et al., *Rapid affinity purification of retinal arrestin (48 kDa protein) via its light-dependent binding to phosphorylated rhodopsin.* FEBS Lett, 1986. **207**(2): p. 292-5.
27. Makino, C.L., X.H. Wen, and J. Lem, *Piecing together the timetable for visual transduction with transgenic animals.* Curr Opin Neurobiol, 2003. **13**(4): p. 404-12.
28. Arshavsky, V.Y. and M.E. Burns, *Photoreceptor signaling: supporting vision across a wide range of light intensities.* J Biol Chem, 2012. **287**(3): p. 1620-6.
29. Najafi, M., N.A. Maza, and P.D. Calvert, *Steric volume exclusion sets soluble protein concentrations in photoreceptor sensory cilia.* Proc Natl Acad Sci U S A, 2012. **109**(1): p. 203-8.
30. Najafi, M., et al., *Impact of signaling microcompartment geometry on GPCR dynamics in live retinal photoreceptors.* J Gen Physiol, 2012. **140**(3): p. 249-66.
31. Calvert, P.D., W.E. Schiesser, and E.N. Pugh, Jr., *Diffusion of a soluble protein, photoactivatable GFP, through a sensory cilium.* J Gen Physiol, 2010. **135**(3): p. 173-96.
32. Bruns, I.R., et al., *A potential novel strategy to separate therapeutic- and side-effects that are mediated via the same receptor: beta-arrestin2/G-protein coupling antagonists.* J Clin Pharm Ther, 2006. **31**(2): p. 119-28.
33. Smith, W.C., et al., *Cloning and functional characterization of salamander rod and cone arrestins.* Invest Ophthalmol Vis Sci, 2000. **41**(9): p. 2445-55.
34. Gurevich, V.V. and J.L. Benovic, *Arrestin: mutagenesis, expression, purification, and functional characterization.* Methods Enzymol, 2000. **315**: p. 422-37.
35. Laemmli, U.K., *Cleavage of structural proteins during the assembly of the head of bacteriophage T4.* Nature, 1970. **227**(5259): p. 680-5.
36. Philp, N.J., W. Chang, and K. Long, *Light-stimulated protein movement in rod photoreceptor cells of the rat retina.* FEBS Lett, 1987. **225**(1-2): p. 127-32.
37. Ralston, G., *Introduction to Analytical Ultracentrifugation*. 1993, Fullerton, CA: Beckman.
38. Hansen, J.C., J. Lebowitz, and B. Demeler, *Analytical ultracentrifugation of complex macromolecular systems.* Biochemistry, 1994. **33**(45): p. 13155-63.
39. Lebowitz, J., M.S. Lewis, and P. Schuck, *Modern analytical ultracentrifugation in protein science: a tutorial review.* Protein Sci, 2002. **11**(9): p. 2067-79.
40. Schuck, P., *Size-distribution analysis of macromolecules by sedimentation velocity ultracentrifugation and lamm equation modeling.* Biophys J, 2000. **78**(3): p. 1606-19.
41. Schuck, P., *On the analysis of protein self-association by sedimentation velocity analytical ultracentrifugation.* Anal Biochem, 2003. **320**(1): p. 104-24.

42. Kroll, K.L. and E. Amaya, *Transgenic Xenopus embryos from sperm nuclear transplantations reveal FGF signaling requirements during gastrulation.* Development, 1996. **122**(10): p. 3173-83.
43. Batni, S., et al., *Xenopus rod photoreceptor: model for expression of retinal genes.* Methods Enzymol, 2000. **316**: p. 50-64.
44. Haeri, M. and B.E. Knox, *Generation of transgenic Xenopus using restriction enzyme-mediated integration.* Methods Mol Biol, 2012. **884**: p. 17-39.
45. Gurdon, J., *Nuclear reprogramming in eggs.* Nat Med, 2009. **15**(10): p. 1141-4.
46. Simpson, R.J., *Stabilization of proteins for storage.* Cold Spring Harb Protoc, 2010. **2010**(5): p. pdb.top79.
47. Koutalos, Y., K. Nakatani, and K.W. Yau, *Cyclic GMP diffusion coefficient in rod photoreceptor outer segments.* Biophys J, 1995. **68**(1): p. 373-82.
48. Korenbrot, J.I. and R.A. Cone, *Dark ionic flux and the effects of light in isolated rod outer segments.* J Gen Physiol, 1972. **60**(1): p. 20-45.
49. Hamm, H.E. and M.D. Bownds, *Protein complement of rod outer segments of frog retina.* Biochemistry, 1986. **25**(16): p. 4512-23.
50. Corless, J.M. and T.G. Schneider, *Patterns of interdisk connections within the lamellar domains of retinal rod outer segment disks: observations relevant to the axial propagation of incisures.* Exp Eye Res, 1987. **45**(6): p. 883-905.
51. Nickell, S., et al., *Three-dimensional architecture of murine rod outer segments determined by cryoelectron tomography.* J Cell Biol, 2007. **177**(5): p. 917-25.
52. Kuhn, H., S.W. Hall, and U. Wilden, *Light-induced binding of 48-kDa protein to photoreceptor membranes is highly enhanced by phosphorylation of rhodopsin.* FEBS Lett, 1984. **176**(2): p. 473-8.
53. Wilden, U., S.W. Hall, and H. Kuhn, *Phosphodiesterase activation by photoexcited rhodopsin is quenched when rhodopsin is phosphorylated and binds the intrinsic 48-kDa protein of rod outer segments.* Proc Natl Acad Sci U S A, 1986. **83**(5): p. 1174-8.
54. Wacker, W.B., et al., *Experimental allergic uveitis. Isolation, characterization, and localization of a soluble uveitopathogenic antigen from bovine retina.* J Immunol, 1977. **119**(6): p. 1949-58.
55. Granzin, J., et al., *X-ray crystal structure of arrestin from bovine rod outer segments.* Nature, 1998. **391**(6670): p. 918-21.
56. Hirsch, J.A., et al., *A Model for Arrestin's Regulation: The 2.8 Å Crystal Structure of Visual Arrestin.* Cell, 1999. **97**(2): p. 257-269.
57. Kim, M., et al., *Conformation of receptor-bound visual arrestin.* Proc Natl Acad Sci U S A, 2012. **109**(45): p. 18407-12.
58. Cole, J.L., et al., *Analytical ultracentrifugation: sedimentation velocity and sedimentation equilibrium.* Methods Cell Biol, 2008. **84**: p. 143-79.
59. Malik, L., et al., *Self-assembly of designed coiled coil peptides studied by small-angle X-ray scattering and analytical ultracentrifugation.* J Pept Sci, 2013. **19**(5): p. 283-92.
60. Pugh, E.N., Jr., B. Falsini, and A.L. Lyubarsky, *The Origin of the Major Rod- and Cone-Driven Components of the Rodent Electroretinogram and the Effect of Age and Light-Rearing History on the Magnitude of These Components*, in *Photostasis and Related Phenomena*, T. Williams and A. Thistle, Editors. 1998, Springer US. p. 93-128.
61. Brann, M.R. and L.V. Cohen, *Diurnal expression of transducin mRNA and translocation of transducin in rods of rat retina.* Science, 1987. **235**(4788): p. 585-7.

62. Whelan, J.P. and J.F. McGinnis, *Light-dependent subcellular movement of photoreceptor proteins.* J Neurosci Res, 1988. **20**(2): p. 263-70.
63. Orisme, W., et al., *Light-dependent translocation of arrestin in rod photoreceptors is signaled through a phospholipase C cascade and requires ATP.* Cell Signal, 2010. **22**(3): p. 447-56.
64. Reidel, B., et al., *The translocation of signaling molecules in dark adapting mammalian rod photoreceptor cells is dependent on the cytoskeleton.* Cell Motil Cytoskeleton, 2008. **65**(10): p. 785-800.
65. McGinnis, J.F., et al., *Cytoskeleton participation in subcellular trafficking of signal transduction proteins in rod photoreceptor cells.* J Neurosci Res, 2002. **67**(3): p. 290-7.
66. Peterson, J.J., et al., *A role for cytoskeletal elements in the light-driven translocation of proteins in rod photoreceptors.* Invest Ophthalmol Vis Sci, 2005. **46**(11): p. 3988-98.
67. Nair, K.S., et al., *Light-Dependent Redistribution of Arrestin in Vertebrate Rods Is an Energy-Independent Process Governed by Protein-Protein Interactions.* Neuron, 2005. **46**(4): p. 555-567.
68. Peet, J.A., et al., *Quantification of the cytoplasmic spaces of living cells with EGFP reveals arrestin-EGFP to be in disequilibrium in dark adapted rod photoreceptors.* J Cell Sci, 2004. **117**(Pt 14): p. 3049-59.
69. Nair, K.S., et al., *Direct binding of visual arrestin to microtubules determines the differential subcellular localization of its splice variants in rod photoreceptors.* J Biol Chem, 2004. **279**(39): p. 41240-8.
70. Hiller, G. and K. Weber, *Radioimmunoassay for tubulin: a quantitative comparison of the tubulin content of different established tissue culture cells and tissues.* Cell, 1978. **14**(4): p. 795-804.
71. Smith, W.C., et al., *Interaction of arrestin with enolase1 in photoreceptors.* Invest Ophthalmol Vis Sci, 2011. **52**(3): p. 1832-40.
72. Huang, S.P., B.M. Brown, and C.M. Craft, *Visual Arrestin 1 acts as a modulator for N-ethylmaleimide-sensitive factor in the photoreceptor synapse.* J Neurosci, 2010. **30**(28): p. 9381-91.
73. Marszalek, J.R., et al., *Genetic Evidence for Selective Transport of Opsin and Arrestin by Kinesin-II in Mammalian Photoreceptors.* Cell, 2000. **102**(2): p. 175-187.
74. Hink, M.A., et al., *Structural dynamics of green fluorescent protein alone and fused with a single chain Fv protein.* J Biol Chem, 2000. **275**(23): p. 17556-60.
75. Shinohara, T., et al., *Primary and secondary structure of bovine retinal S antigen (48-kDa protein).* Proc Natl Acad Sci U S A, 1987. **84**(20): p. 6975-9.

CHAPTER 3 GENERAL CONCLUSION AND FUTURE DIRECTIONS

Many genetic mutations, which lead to blindness, deafness, mental retardation, kidney disease and other related maladies, result from the improper transport and localization of proteins to sensory and primary cilia [1, 2]. Study on the arrestin self-association property and the mechanism of phototransduction proteins transport is of critical clinical significance on retinal diseases, especially progressive visual loss caused by retinitis pigmentosa and photoreceptor degeneration [3, 4]. Understanding the mechanism of light-driven movement of phototransduction protein in rod photoreceptors provide the information on the causes of blindness and lay the foundation for new therapeutic methods, which could therefore slow the photoreceptor degeneration [5]. Drugs and therapeutic methods could be designed to correct the improper protein translocation and distribution [6]. Moreover, research on the protein transport through the cilia is critical for understanding photoreceptor survival and mechanisms of ciliopathic diseases [7].

Bovine visual arrestin has been discovered to form oligomers at physiological concentrations via sedimentation equilibrium analysis and small-angle X-ray scattering experiments [8-12]. But different results were obtained, with the data fitted to either monomer-dimer equilibrium model [11, 12] or monomer-dimer-tetramer model [8-10]. Kim et al also found that mouse visual arrestin self-associates, with the existence of a monomer-dimer-tetramer equilibrium [8]. One of the most accurate methods to determine the protein hydrodynamic and thermodynamic properties is the analytical ultracentrifugation [13]. With the access of this method at SUNY Upstate Medical University, sedimentation velocity experiment, which belongs to one of the AUC methods, was performed with the collaboration of Dr. Michael Cosgrove's

laboratory. In this study, therefore, we experimentally and theoretically confirmed the self-association property in bovine and mouse visual arrestin via analytical ultracentrifugation experiment, and the feasibility of performing sedimentation velocity experiment in determining the oligomerization of proteins.

Specifically, with a number of advantages, especially on large rod photoreceptor outer segment [14, 15], *Xenopus laevis* had been used extensively as a favorite experimental model in the retinal research [16-18]. To the best of our knowledge, this is the first attempt to provide the oligomerization information of *Xenopus* visual arrestin, demonstrating that visual arrestin self-association is not only a common feature of mammalian visual arrestin, but also exists in amphibian animals including *Xenopus laevis*. Besides, we also explored whether self-association could be impaired by site-directed mutagenesis (F78A, Y84A and F193A), and found that these mutations did not cause constitutively monomeric form, indicating for the first time that these regions which were crucial for mammalian arrestin self-association, were not conserved in *Xenopus* arrestin. Most importantly, results revealed that the data was fitted to monomer-dimer equilibrium model, which challenged the monomer-dimer-tetramer model. In addition, the dimer percentage is at least 2-fold higher than the monomer percentage in all four arrestin types at physiological concentrations. The mechanism for the light-driven translocation of arrestin to the outer segment was suggested to involve free diffusion with binding affinity of light-activated phosphorylated rhodopsin, and we hypothesized that the translocation to the inner segment was via steric volume exclusion [19]. Together, our results established the foundation for this hypothesis, and the dynamic arrestin self-association and steric volume exclusion might be adequate as the explanation for the distribution pattern of visual arrestin in dark-adapted state.

Future research directions related to this project were suggested in this chapter.

- ***Activity of arrestin and its oligomerization in living cells***

The result of my study demonstrated that bovine and mouse arrestins were fitted to MD model with the dissociation constants of 736.4 μM and 1127.0 μM, respectively. The data was different from the published paper using muliangle laser scattering , in which the two species of arretins were fitted to MDT model with $K_{D,dim}$=37.2 μM and $K_{D,tet}$=7.4 μM for bovine arrestin, and $K_{D,dim}$=57.5 μM and $K_{D,tet}$=63.1 μM for mouse arrestin [8]. Firsty, the result of scattering experiment is sensitive to the contamination in the tested sample, however, analytical ultracentrifugation can reduce the impact of contamination by choosing the exact peak of arrestin. Secondly, the highest concentration in previous paper was only 20 μM and then extrapolated to higher concentrations. However, the highest concentrations obtained in my study was ~100 μM for bovine arrestin and ~200 μM for mouse arrestin. Thirdly, in my study, it was possible that unfolded arrestin, which was in inactive state, existed as well, leading to inaccurate measurement of the arrestin concentration with the UV-Vis spectrophotometer and therefore affecting the fitting to the models and the dissociation constants. Only active arrestin could form oligomers, so the following study will test the activity of arrestin by measuring its binding affinity to phosphorylated photoactivated rhodopsin. Method of size-exclusion chromatography could also be performed in order to get rid of the unfolded arrestin which forms large soluble aggregates, although these large species of proteins have not found in my gels yet.

While the hypothesis potentially answers the long-existing question in photoreceptor physiology, it raises new challenges that need further exploration. Visual arrestin forms oligomers at physiological concentrations in vitro; however, whether it can oligomerize in living cells as well is unclear. And if so, it is obscure that in which subcellular compartments this oligomerization could occur in living cells and under what conditions and concentration range,

the self-association could happen. Further investigation will also be needed to determine *in vivo* how oligomerization impacts arrestin distribution pattern in rod subcellular compartments. How self-association affects the light-driven movement of arrestin needs to be examined as well.

- ***Influence of transducin subunits to protein distribution and their mobility***

In the dark-adapted state, transducin is proposed to localize in the rod outer segment as the αβγ complex because its sufficient binding affinity to disc membranes due to the myristoyl on α subunit and the farnesyl group on βγ subunits [20-25]. The mechanism for the light-driven transducin movement to the inner segment is considered as the reduced membranous binding affinity because of the dissociation of α subunit and βγ subunits. However, neither of the hypotheses has been proved yet, and therefore it is necessary to study the influence of individual transducin subunits to protein distribution and their mobility. Meanwhile the impact of αβγ complex on mobility and the distribution pattern needs to be further studied, as does whether there is any interplay between the theory of steric volume exclusion and membrane affinity on transducin distribution pattern.

Reference

1. Valastyan, J.S. and S. Lindquist, *Mechanisms of protein-folding diseases at a glance.* Dis Model Mech, 2014. **7**(1): p. 9-14.
2. Morrissette, J.D., R.P. Colliton, and N.B. Spinner, *Defective intracellular transport and processing of JAG1 missense mutations in Alagille syndrome.* Hum Mol Genet, 2001. **10**(4): p. 405-13.
3. Farrar, G.J., et al., *Autosomal dominant retinitis pigmentosa: linkage to rhodopsin and evidence for genetic heterogeneity.* Genomics, 1990. **8**(1): p. 35-40.
4. Fahim AT, D.S., Weleber RG, *Retinitis Pigmentosa Overviewji.* GeneReviews™ [Internet], 1993.
5. Vishnivetskiy, S.A., et al., *Engineering visual arrestin-1 with special functional characteristics.* J Biol Chem, 2013. **288**(5): p. 3394-405.
6. Hung, M.C. and W. Link, *Protein localization in disease and therapy.* J Cell Sci, 2011. **124**(Pt 20): p. 3381-92.
7. Calvert, P.D., W.E. Schiesser, and E.N. Pugh, Jr., *Diffusion of a soluble protein, photoactivatable GFP, through a sensory cilium.* J Gen Physiol, 2010. **135**(3): p. 173-96.
8. Kim, M., et al., *Robust self-association is a common feature of mammalian visual arrestin-1.* Biochemistry, 2011. **50**(12): p. 2235-42.
9. Hanson, S.M., et al., *Structure and function of the visual arrestin oligomer.* EMBO J, 2007. **26**(6): p. 1726-36.
10. Imamoto, Y., et al., *Concentration-Dependent Tetramerization of Bovine Visual Arrestin.* Biophysical Journal, 2003. **85**(2): p. 1186-1195.
11. Schubert, C., et al., *Visual arrestin activity may be regulated by self-association.* J Biol Chem, 1999. **274**(30): p. 21186-90.
12. Shilton, B.H., et al., *The solution structure and activation of visual arrestin studied by small-angle X-ray scattering.* Eur J Biochem, 2002. **269**(15): p. 3801-9.
13. Ralston, G., *Introduction to Analytical Ultracentrifugation*. 1993, Fullerton, CA: Beckman.
14. Xiong, W.H. and K.W. Yau, *Rod sensitivity during Xenopus development.* J Gen Physiol, 2002. **120**(6): p. 817-27.
15. Moritz, O.L., et al., *Fluorescent photoreceptors of transgenic Xenopus laevis imaged in vivo by two microscopy techniques.* Invest Ophthalmol Vis Sci, 1999. **40**(13): p. 3276-80.
16. Papermaster, D.S. and W.J. Dreyer, *Rhodopsin content in the outer segment membranes of bovine and frog retinal rods.* Biochemistry, 1974. **13**(11): p. 2438-44.
17. Papermaster, D.S., C.A. Converse, and J. Siuss, *Membrane biosynthesis in the frog retina: opsin transport in the photoreceptor cell.* Biochemistry, 1975. **14**(7): p. 1343-52.
18. Papermaster, D.S., et al., *Immunocytochemical localization of a large intrinsic membrane protein to the incisures and margins of frog rod outer segment disks.* J Cell Biol, 1978. **78**(2): p. 415-25.
19. Najafi, M., N.A. Maza, and P.D. Calvert, *Steric volume exclusion sets soluble protein concentrations in photoreceptor sensory cilia.* Proc Natl Acad Sci U S A, 2012. **109**(1): p. 203-8.
20. Nair, K.S., et al., *Light-Dependent Redistribution of Arrestin in Vertebrate Rods Is an Energy-Independent Process Governed by Protein-Protein Interactions.* Neuron, 2005. **46**(4): p. 555-567.
21. Sokolov, M., et al., *Massive Light-Driven Translocation of Transducin between the Two Major Compartments of Rod Cells: A Novel Mechanism of Light Adaptation.* Neuron, 2002. **34**(1): p. 95-106.
22. Sokolov, M., et al., *Phosducin facilitates light-driven transducin translocation in rod photoreceptors. Evidence from the phosducin knockout mouse.* J Biol Chem, 2004. **279**(18): p. 19149-56.
23. Zhang, H., et al., *UNC119 is required for G protein trafficking in sensory neurons.* Nat Neurosci, 2011. **14**(7): p. 874-80.

24. Kassai, H., et al., *Farnesylation of retinal transducin underlies its translocation during light adaptation.* Neuron, 2005. **47**(4): p. 529-39.
25. Kerov, V., et al., *Transducin activation state controls its light-dependent translocation in rod photoreceptors.* J Biol Chem, 2005. **280**(49): p. 41069-76.